

The non-intrusive reduced basis two-grid method applied to sensitivity analysis

January 18, 2023

Elise Grosjean ¹, Bernd Simeon ¹

Abstract

This paper deals with the derivation of Non-Intrusive Reduced Basis (NIRB) techniques for sensitivity analysis, more specifically the direct and adjoint state methods. For highly complex parametric problems, these two approaches may become too costly. To reduce computational times, Proper Orthogonal Decomposition (POD) and Reduced Basis Methods (RBMs) have already been investigated. The majority of these algorithms are however intrusive in the sense that the High-Fidelity (HF) code must be modified. To address this issue, non-intrusive strategies are employed. The NIRB two-grid method uses the HF code solely as a “black-box”, requiring no code modification. Like other RBMs, it is based on an offline-online decomposition. The offline stage is time-consuming, but it is only executed once, whereas the online stage is significantly less expensive than an HF evaluation.

In this paper, we propose new NIRB two-grid algorithms for both the direct and adjoint state methods.

On the direct method, we prove on a classical model problem, the heat equation, that HF evaluations of sensitivities reach an optimal convergence rate in $L^\infty(0, T; H^1(\Omega))$, and then establish that these rates are recovered by the proposed NIRB approximation. These results are supported by numerical simulations. We then numerically demonstrate that a Gaussian process regression can be used to approximate the projection coefficients of the NIRB two-grid method. This further reduces the computational costs of the online step while only computing a coarse solution of the initial problem. All numerical results are run with the model problem as well as a more complex problem, namely the Brusselator system.

1 Introduction.

Sensitivity analysis is a critical step in optimizing the parameters of a parametric model. The goal is to see how sensitive its results are to small changes of its input parameters. It is especially useful in the biomedical field when experiments are extremely complex or prohibitively expensive. Indeed, conducting several experiments to determine the impact of all parameters involved in biological processes may be difficult, if not impossible.

Several methods have been developed for computing sensitivities, see [4] for an overview. We focus here on two differential-based sensitivity analysis approaches in connection with models given as reaction-diffusion equations.

- “The direct method”, also known as the “forward method”, which may be used when dealing with discretized solutions of parametric Partial Differential Equations (PDEs). The sensitivities (of the solution or other outputs of interest) are computed directly from the original problem. One drawback is that it necessitates solving a new system for each parameter of interest, i.e., for P parameters of interest, $P + 1$ problems have to be solved.
- “The adjoint state method”, also known as the “backward method”. It may be a viable option [50] when the direct method becomes prohibitively expensive. In this setting, the goal is to compute the sensitivities of an objective function that one aims at minimizing. The associated Lagrangian is formulated, and by choosing appropriate multipliers, a new system known as “the adjoint” is derived. This approach is preferred in many situations since it avoids calculating the sensitivities with respect to the solutions. For example,

¹Felix-Klein-Institut für Mathematik, Kaiserslautern TU, 67657, Deutschland

in the framework of inverse problems, one can determine the “true” parameter from several measures (which are frequently provided by multiple sensors) while combining it with a gradient-type optimization algorithm. As a result, we get the “integrated effects” on the outputs over a time interval. The advantage is that it only requires two systems to solve regardless of the number of parameters of interest.

Thus, the direct method is appealing when there are relatively few parameters or a large number of objective functions, whereas the adjoint state method is preferred when there are many parameters and few objective functions.

Earlier works. For extremely complex simulations, both methods may still be impractical. Several reduction techniques have thus been investigated in order to reduce the complexity of the sensitivity computation. Among them, Reduced Basis Methods (RBMs) are a well-developed field [40, 46, 3]. They use an offline-online decomposition, in which the offline step is time-consuming but is only performed once, and the online step is significantly less expensive than a High-Fidelity (HF) evaluation. In the context of sensitivity analysis, the majority of these studies rely on a Galerkin projection onto the adjoint state system in the online part. In what follows, we present a brief review of previous works on RBMs combined with both sensitivity methods.

- Let us begin with the direct method. It has been employed and studied with RB spaces in various applications, e. g., [45, 53, 13]). The sensitivities may also be useful to enhance the reduced state approximation. Unlike the other studies cited below, the sensitivities in [28] are computed to improve RB methods (see also [27] with a Lagrangian formulation or [26] with a finite difference approach [26]). Still to improve an approximation, in [34], a combined method is proposed (based on local and global approximations with series expansion and a RB expression), which was first developed in [33]. Note also that variance-based sensitivity analysis has been investigated using RBMs [31] and non-intrusive RB [38].
- The adjoint state formulation can be thought of as a PDE-constrained optimization. The first applications of this method in conjunction with computational reduction approaches can be found in [30] in the context of RBMs, where several RB sub-spaces are compared or in [48] with the POD method, with an affine parameter dependence. Currently, particular emphasis is being placed on developing accurate a-posteriori error estimates in order to improve basis generation [47, 52, 11, 12] with Proper Orthogonal Decomposition (POD) and/or RBMs.

RBMs and POD have also been investigated in the context of optimal control under uncertainty [9]. In recent studies, the case of infinite-dimensional control function is considered with RB approximations on the state, adjoint, and control variables [32, 1]. Even if the adjoint state method is frequently preferred, writing its associated reduced problem can be difficult when the adjoint formulation is not straightforward. It may also be reformulated to take advantage of previously developed RB theory. For example, in [43], it is rewritten as a saddle-point problem for Stokes-type problems.

To conclude this brief overview of RBMs applied to sensitivity analysis, we add that non-intrusive methods have been developed, in the framework of the inverse problem, without computing the sensitivities (see the PBDW method [41, 25, 10] with a direct formulation).

Motivation. Even though the Galerkin projection is prevalent in the literature, its main disadvantage lies in its intrusiveness. Indeed, in order to approximate the solution of a PDE, the matrices computed from its variational formulation must be changed in the HF code. This may be difficult if the HF is very complex or even impossible if it has been purchased, as is often the case in an industrial context. From an engineering standpoint, Non-Intrusive Reduced Basis (NIRB) methods are more practical to implement than intrusive RBMs because they only require the execution of the HF code as a “black-box” solver. Apparently, NIRB methods have not yet been used to approximate sensitivities except for statistical approaches such as variance-based sensitivity analysis.

In this paper, we aim at computing the sensitivities with respect to some parameters of interest $\mu \in \mathcal{G}$, with the direct and adjoint methods combined with NIRB techniques. We focus on the NIRB two-grid method [7, 18, 8, 49] (see also different NIRB methods [6, 2, 16] from the two-grid method). Like most RBMs, the NIRB two-grid method relies on the assumption that the manifold of all solutions $\mathcal{S} = \{u(\mu), \mu \in \mathcal{G}\}$ has a small Kolmogorov width [36] (in what follows, $u_h(\mu)$ will refer to the HF solution for the parameter μ).

The two-grid algorithm can be employed for a variety of PDEs and is simple to implement. It has been studied with FEM in the context of elliptic equations [7] and parabolic equations [20] (see also [18] for finite

volume schemes). Furthermore, because it is non-intrusive, it is suitable for a wide range of problems. The effectiveness of this method relies on its offline/online decomposition (as most RBMs). The offline part is time-consuming but it is only performed once. On the contrary, the specific feature of the NIRB approach is to solve the parametric problem on a coarse mesh only during the online step, and then to rapidly improve the precision of the coarse solution. It makes this portion of the algorithm much cheaper than a HF evaluation.

In this paper, we combine the two-grids framework with both sensitivity analysis methods. Then, drawing inspiration from two recent works [19, 21], we efficiently apply a supervised learning process to further reduce the computational cost of its online stage with the direct method, in the context of parabolic equations. During the online stage, this additional step allows us to solve only the initial problem on the coarse mesh, regardless of the number of parameters of interest, making this novel approach very appealing. We highlight the fact that because the direct approach requires a new system to be solved for each parameter, the adjoint method is preferred in many studies (as cited above), despite the fact that its formulation is more complex and yields integrated sensitivities over time.

Outline of the paper. This article is about extending the NIRB two-grid method to the computation of sensitivities and performing the associated numerical analysis. We present and illustrate the NIRB algorithms applied to both sensitivity analysis methods with several numerical results. With the direct method, we have carried out a thorough theoretical analysis of the heat equation as model problem. In this setting, we have optimal convergence rates in $L^\infty(0, T; H^1(\Omega))$ for the spatial HF semi-discretized sensitivity solution and for its fully-discretized form. It turns out that we obtain theoretically and numerically these optimal rates also for the NIRB sensitivity approximations, provided that the initial approximations are correctly constructed. Our main theoretical result is given by Theorem 4.1.

The rest of this paper is organized as follows. Section 2 describes both sensitivity methods along with established convergence results and the NIRB two-grid algorithm for parabolic equations. In Section 3, we present the algorithms for the direct and adjoint methods with the NIRB two-grid approach, as well as the new version of the algorithm for the direct method. Section 4 is devoted to the theoretical results on the rate of convergence for the NIRB sensitivity approximation. In the last section 5, several numerical results are presented and illustrate the theoretical ones.

2 Mathematical Background.

Let Ω be a bounded domain in \mathbb{R}^d , with $d \leq 3$ and a smooth enough boundary $\partial\Omega$, and consider a parametric problem \mathcal{P} on Ω . For the NIRB two-grid method, we consider two spatial "grids" of Ω :

- one fine mesh, denoted \mathcal{T}_h , where its size h is defined as

$$h = \max_{K \in \mathcal{M}_h} h_K, \quad (1)$$

- and on coarse mesh, denoted \mathcal{T}_H , with its size defined as

$$H = \max_{K \in \mathcal{M}_H} H_K \gg h, \quad (2)$$

where the diameter h_K (or H_K) of any element K in a mesh is equal to $\sup_{x, y \in K} |x - y|$.

In this section, we first introduce our model problem, that of the heat equation, in a continuous setting, and then its spatial (over the two meshes) and time discretizations. Then, we recall the NIRB algorithm in the context of parabolic equations, and finally, we detail the sensitivity problems associated to the heat equation.

In the next sections, C will denote various positive constants independent of the size of the meshes h and H and of the parameter μ , and $C(\mu)$ will denote constants independent of the sizes of the meshes h and H but dependent of μ .

2.1 A model problem: The heat equation.

2.1.1 The continuous problem.

We consider the following heat equation on the domain Ω with homogeneous Dirichlet conditions, which takes the form

$$\begin{cases} u_t - \nabla \cdot (A(\mu) \nabla u) = f, & \text{in } \Omega \times]0, T], \\ u(\cdot, 0; \mu) = u^0(\cdot; \mu), & \text{in } \Omega, \\ u(\cdot, t) = 0, & \text{on } \partial\Omega \times]0, T], \end{cases} \quad (3)$$

where

$$f \in L^2(\Omega \times [0, T]), \text{ while } u^0(\mu) \in H_0^1(\Omega) \text{ and } \mu = (\mu_1, \dots, \mu_P) \in \mathcal{G} \subset \mathbb{R}^P \text{ is the parameter, such that } A : \Omega \times \mathcal{G} \rightarrow \mathcal{M}_d(\mathbb{R}) \text{ is measurable, bounded, and uniformly elliptic.} \quad (4)$$

For any $t > 0$, the solution $u(\cdot, t) \in H_0^1(\Omega)$, and $u_t(\cdot, t) \in L^2(\Omega)$ stands for the derivative of u with respect to time.

We use the conventional notations for space-time dependent Sobolev spaces [39]

$$\begin{aligned} L^p(0, T; V) &:= \{u(\mathbf{x}, t) \mid \|u\|_{L^p(0, T; V)} := \left(\int_0^T \|u(\cdot, t)\|_V^p dt \right)^{1/p} < \infty\}, \quad 1 \leq p < \infty, \\ L^\infty(0, T; V) &:= \{u(\mathbf{x}, t) \mid \|u\|_{L^\infty(0, T; V)} := \text{ess sup}_{0 \leq t \leq T} \|u(\cdot, t)\|_V < \infty\}, \end{aligned}$$

where V is a real Banach space with norm $\|\cdot\|_V$. The variational form of (3) is given by:

$$\begin{cases} \text{Find } u \in L^2(0, T; H_0^1(\Omega)) \text{ with } u_t \in L^2(0, T; H^{-1}(\Omega)) \text{ such that} \\ (u_t(t, \cdot), v) + a(u(t, \cdot), v; \mu) = (f(t, \cdot), v), \quad \forall v \in H_0^1(\Omega) \text{ and } t \in (0, T), \\ u(\cdot, 0; \mu) = u^0(\cdot; \mu), \text{ in } \Omega, \end{cases} \quad (5)$$

where a is given by

$$a(w, v; \mu) = \int_\Omega A(\mathbf{x}; \mu) \nabla w(\mathbf{x}) \cdot \nabla v(\mathbf{x}) d\mathbf{x}, \quad \forall w, v \in H_0^1(\Omega). \quad (6)$$

We remind that (5) is well posed (see [15] for the existence and the uniqueness of solutions to problem (5)) and we refer to the notations of [15]. Note that we will use the notation (\cdot, \cdot) to denote the classical L^2 -inner product on Ω .

2.1.2 The various discretizations.

For the NIRB algorithm, we use the two spatial grids on the variational formulation (5) of our problem (3). We employed \mathbb{P}_1 finite elements to discretize in space. Thus, we introduce V_h and V_H , the continuous piecewise linear finite element functions (on fine and coarse meshes, respectively) that vanish on the boundary $\partial\Omega$. We consider the so-called Ritz projection operator $P_h^1 : H_0^1(\Omega) \rightarrow V_h$ (P_H^1 on V_H is defined similarly) which is given by

$$(\nabla P_h^1 u, \nabla v) = (\nabla u, \nabla v), \quad \forall v \in V_h, \text{ for } u \in H_0^1(\Omega). \quad (7)$$

In the context of time-dependent problems, a time stepping method of finite difference type is used to get a fully discrete approximation of the solution of (3). As for the spatial domain, we consider two different time grids:

- One time grid, denoted F , is associated to fine solutions (for the generation of the snapshots). To avoid making notations more cumbersome, we will consider a uniform time step Δt_F . The time levels can be written $t^n = n \Delta t_F$, where $n \in \mathbb{N}^*$.
- Another time grid, denoted G , is used for coarse solutions. By analogy with the fine grid, we consider a uniform grid with time step Δt_G . Now, the time levels are written $\tilde{t}^m = m \Delta t_G$, where $m \in \mathbb{N}^*$.

As in the elliptic context [7], the NIRB algorithm is designed to recover the optimal estimate in space. To do so, the NIRB theory uses Aubin-Nitsche lemma in the context of FEM. Yet, since there is no such argument as the Aubin-Nitsche lemma for time stepping methods, we must consider time discretizations that provide the same precision with larger time steps, as detailed in [20]. Thus, we consider a higher order time scheme for the coarse solution. As in [20], we used an Euler scheme (first order approximation) for the fine solution and the Crank-Nicolson scheme (second order approximation) for the coarse solution on our model problem. Thus, we deal with two kinds of notations for the discretized solutions:

- $u_h(\mathbf{x}, t)$ and $u_H(\mathbf{x}, t)$ (or $u_h(\mathbf{x}, t; \mu)$ and $u_H(\mathbf{x}, t; \mu)$ in order to highlight the μ -dependency) that respectively denote the fine and coarse solutions of the spatially semi-discrete solution, at time $t \geq 0$.
- $u_h^n(\mathbf{x})$ and $u_H^m(\mathbf{x})$ (or $u_h^n(\mathbf{x}; \mu)$ and $u_H^m(\mathbf{x}; \mu)$) that respectively denote the fine and coarse full-discretized solutions at time $t^n = n \times \Delta t_F$ and $\tilde{t}^m = m \times \Delta t_G$.

Remark 2.1. To simplify notations, we consider that both time grids end at time T here,

$$T = N_T \Delta t_F = M_T \Delta t_G.$$

The semi-discrete form of the variational problem (5) writes for the fine mesh (similarly for the coarse mesh):

$$\left\{ \begin{array}{l} \text{Find } u_h(t) = u_h(\cdot, t) \in V_h \text{ for } t \in [0, T] \text{ such that} \\ (u_{h,t}(t), v_h) + a(u_h(t), v_h; \mu) = (f(t), v_h), \forall v_h \in V_h \text{ and } t \in]0, T], \\ u_h(\cdot, 0; \mu) = u_h^0(\cdot; \mu) = P_h^1(u^0)(\cdot; \mu). \end{array} \right. \quad (8)$$

From the definition of the Ritz projection operator P_h^1 (7), the initial condition $u_h^0(\mu)$ (and similarly for the coarse mesh) is such that

$$(\nabla u_h^0(\mu), \nabla v_h) = (\nabla u^0(\mu), \nabla v_h), \forall v_h \in V_h, \quad (9)$$

and hence, it corresponds to the finite element approximation of the corresponding elliptic problem whose exact solution is $u^0(\mu)$.

The full discrete form of the variational problem (5) for the fine mesh with an implicit Euler scheme writes:

$$\left\{ \begin{array}{l} \text{Find } u_h^n \in V_h \text{ for } n = 0, \dots, N_T \text{ such that} \\ (\bar{\partial} u_h^n, v_h) + a(u_h^n, v_h; \mu) = (f(t^n), v_h), \forall v_h \in V_h \text{ and } n = 1, \dots, N_T, \\ u_h(\cdot, 0; \mu) = u_h^0(\cdot; \mu), \end{array} \right. \quad (10)$$

where the time derivative in the variational form of the problem (8) has been replaced by a backward difference quotient, $\bar{\partial} u_h^n = \frac{u_h^n - u_h^{n-1}}{\Delta t_F}$.

For the coarse mesh with the Crank-Nicolson scheme, and with the notation $\bar{\partial} u_H^m = \frac{u_H^m - u_H^{m-1}}{\Delta t_G}$, it becomes:

$$\left\{ \begin{array}{l} \text{Find } u_H^m \in V_H \text{ for } m = 0, \dots, M_T, \text{ such that} \\ (\bar{\partial} u_H^m, v_H) + a\left(\frac{u_H^m + u_H^{m-1}}{2}, v_H; \mu\right) = (f(\tilde{t}^{m-\frac{1}{2}}), v_H), \forall v_H \in V_H \text{ and } m = 1, \dots, M_T, \\ u_H(\cdot, 0; \mu) = u_H^0(\cdot; \mu), \end{array} \right. \quad (11)$$

where $\tilde{t}^{m-\frac{1}{2}} = \frac{\tilde{t}^m + \tilde{t}^{m-1}}{2}$.

To approximate the solution $u(\mu)$ with the NIRB two-grid method, as explained in [20], we will need to interpolate in space (as for elliptic equations) and in time the coarse solution. So let us introduce the quadratic interpolation in time of a coarse solution at time $t^n \in I_m = [\tilde{t}^{m-1}, \tilde{t}^m]$ defined on $[\tilde{t}^{m-2}, \tilde{t}^m]$ from the coarse approximations at times $\tilde{t}^{m-2}, \tilde{t}^{m-1}$, and \tilde{t}^m , for all $m = 2, \dots, M_T$. To this purpose, we employ the following parabola on $[\tilde{t}^{m-2}, \tilde{t}^m]$:

For $m \geq 2$, $\forall n \in I_m = [\tilde{t}^{m-1}, \tilde{t}^m]$,

$$\begin{aligned} I_n^2[u_H^m](\mu) := & \frac{u_H^{m-2}(\mu)}{(\tilde{t}^m - \tilde{t}^{m-2})(\tilde{t}^{m-2} - \tilde{t}^{m-1})} \left[-(t^n)^2 + (\tilde{t}^{m-1} + \tilde{t}^m)t^n - t^{m-1}t^m \right] \\ & + \frac{u_H^{m-1}(\mu)}{(\tilde{t}^{m-2} - \tilde{t}^{m-1})(\tilde{t}^{m-1} - \tilde{t}^m)} \left[-(t^n)^2 + (\tilde{t}^m + \tilde{t}^{m-2})t^n - t^m t^{m-2} \right] \\ & + \frac{u_H^m(\mu)}{(\tilde{t}^{m-1} - \tilde{t}^m)(\tilde{t}^m - \tilde{t}^{m-2})} \left[-(t^n)^2 + (\tilde{t}^{m-2} + \tilde{t}^{m-1})t^n - t^{m-2}t^{m-1} \right]. \end{aligned} \quad (12)$$

For $t^n \in I_1 = [\tilde{t}^0, \tilde{t}^1]$, we use the same parabola defined by the coarse approximations at times \tilde{t}^0 , \tilde{t}^1 , \tilde{t}^2 as the one used over $[\tilde{t}^1, \tilde{t}^2]$. We denote by $\hat{u}_H^n(\mu) = I_n^2[u_H^m](\mu)$ the quadratic interpolation of u_H^m at a time n . Note that we choose this interpolation in order to keep an approximation of order 2 in time Δt_G (it works also with other quadratic interpolations).

In the next section, we recall the NIRB algorithm in the context of parabolic equations.

2.2 Reminders on the Non-Intrusive Reduced Basis method (NIRB) in the context of parabolic equations.

Let $u(\mu)$ be the exact solution of problem (3) for a parameter $\mu \in \mathcal{G}$. With the NIRB algorithm, we aim at quickly approximating this solution by using a reduced space, denoted X_h^N , constructed from N fully discretized solutions of (10), namely the so-called snapshots. Since each snapshot is a HF finite element approximation in space at a time t^n , $n = 0, \dots, N_T$ (N_T being potentially very high), not all of the time steps may be required for the construction of the reduced space. Let N refer to the number of snapshots employed for the RB construction and N_μ be the corresponding number of parameters used. For each parameter μ_i , $i = 1, \dots, N_\mu$, selected during the RB generation, the associated number of time steps employed is denoted N^i . Thus, the RB space is defined as

$$X_h^N := \text{Span}\{u_h^{(n_j)i}(\mu_i) \mid (n_j)_i \subset \{0, \dots, N_T\}, i = 1, \dots, N_\mu, j = 1, \dots, N^i\}, \quad (13)$$

with $N := \sum_{i=1}^{N_\mu} N^i$.

We now recall the offline/online decomposition of the NIRB two-grid procedure with parabolic equations:

- “Offline step”

The offline part of the algorithm allows us to construct the reduced space X_h^N .

1. From training parameters $(\mu_i)_{i \in \{1, \dots, N_{\text{train}}\}}$, we define $\mathcal{G}_{\text{train}} = \bigcup_{i \in \{1, \dots, N_{\text{train}}\}} \mu_i$. Then, in order to construct the RB, we employ a greedy procedure which adequately choose the parameters $(\mu_i)_{i=1, \dots, N_\mu}$ within $\mathcal{G}_{\text{train}}$. This procedure is described in the algorithm 1 (with the setting $N_\mu = N$ to simplify notations). Note that a POD-greedy algorithm may also be employed [20, 24, 23, 35].

Remark 2.2. *The greedy algorithm is usually less expensive than the POD-greedy (thanks to a-posteriori error estimates). Yet, in case the snapshots are computed for all time steps as it is required here, the latter is more reasonable. Our choice of using a greedy procedure is motivated by the fact that it is more efficient with the post-treatment introduced below.*

The RB time-independent functions, denoted $(\Phi_i^h)_{i=1, \dots, N}$, are generated at the end of this step from fine fully-discretized solutions $\{u_h^n(\mu_i)\}_{i \in \{1, \dots, N_\mu\}, n \in \{0, \dots, N_T\}}$ by solving problem (10) with the HF solver. Note that even if all the time steps are computed, only N^i are used for each $i \in \{1, \dots, N_\mu\}$ in the RB construction. Since at each step k of the procedure, all sets added in the RB are in the orthogonal complement of X_h^{k-1} , it yields an L^2 orthogonal basis without further processing. Hence, X_h^N can be defined as $X_h^N = \text{Span}\{\Phi_1^h, \dots, \Phi_N^h\}$, with $(\Phi_i^h)_{i=1, \dots, N}$ L^2 -orthonormalized functions.

Remark 2.3. *In practice, the algorithm is halted with a stopping criterion such as an error threshold or a maximum number of basis functions to generate.*

Algorithm 1 Greedy algorithm

Input: tol , $\{u_h^n(\mu_1), \dots, u_h^n(\mu_{N_{train}})\}$ with $\mu_i \in \mathcal{G}_{train}$, $n = 0, \dots, N_T$.

Output: Reduced basis $\{\Phi_1^h, \dots, \Phi_N^h\}$.

Choose $\mu_1, n_1 = \arg \max_{\mu \in \mathcal{G}_{train}, n \in \{0, \dots, N_T\}} \|u_h^n(\mu)\|_{L^2(\Omega)}$,

Set $\Phi_1^h = \frac{u_h^{n_1}(\mu_1)}{\|u_h^{n_1}(\mu_1)\|_{L^2}}$

Set $\mathcal{G}_1 = \{\mu_1, n_1\}$ and $X_h^1 = \text{span}\{\Phi_1^h\}$.

for $k = 2$ to N **do**:

$\mu_k, n_k = \arg \max_{(\mu, n) \in (\mathcal{G}_{train} \times \{0, \dots, N_T\}) \setminus \mathcal{G}_{k-1}} \|u_h^n(\mu) - P^{k-1}(u_h^n(\mu))\|_{L^2}$, with $P^{k-1}(u_h^n(\mu)) := \sum_{i=1}^{k-1} (u_h^n(\mu), \Phi_i^h) \Phi_i^h$.

Compute $\widetilde{\Phi}_k^h = u_h^{n_k}(\mu_k) - P^{k-1}(u_h^{n_k}(\mu_k))$ and set $\Phi_k^h = \frac{\widetilde{\Phi}_k^h}{\|\widetilde{\Phi}_k^h\|_{L^2(\Omega)}}$

Set $\mathcal{G}_k = \mathcal{G}_{k-1} \cup \{\mu_k\}$ and $X_h^k = X_h^{k-1} \oplus \text{span}\{\Phi_k^h\}$

Stop when $\|u_h^n(\mu) - P^{k-1}(u_h^n(\mu))\|_{L^2} \leq tol$, $\forall \mu \in \mathcal{G}_{train}$, $\forall n = 0, \dots, N_T$.

end for

2. Then, we solve the following eigenvalue problem:

$$\begin{cases} \text{Find } \Phi^h \in X_h^N, \text{ and } \lambda \in \mathbb{R} \text{ such that:} \\ \forall v \in X_h^N, \int_{\Omega} \nabla \Phi^h \cdot \nabla v \, d\mathbf{x} = \lambda \int_{\Omega} \Phi^h \cdot v \, d\mathbf{x}, \end{cases} \quad (14)$$

We get an increasing sequence of eigenvalues λ_i , and orthogonal eigenfunctions $(\Phi_i^h)_{i=1, \dots, N}$, which do not depend on time, orthonormalized in $L^2(\Omega)$ and orthogonalized in $H^1(\Omega)$. Note that with the Gram-Schmidt procedure of the classical greedy algorithm 1, we only obtain an L^2 -orthonormalized RB. As a result, it stabilizes the NIRB approximation with respect to N , as described in [20].

3. We remark that for any parameter μ_k , $k = 1, \dots, N_{\mu}$, the classical NIRB approximation differs from the HF $u_h(\mu_k)$ computed in the offline stage [20]. Thus, to improve NIRB accuracy, we use a “rectification post-processing”. To this purpose, we construct a rectification matrix denoted \mathbf{R}^n for each fine time step $n = 0, \dots, N_T$. This matrix is built from the HF snapshots u_h^n , $n = 0, \dots, N_T$ and coarse snapshots generated by solving (11) and whose parameters are the same as for the fine snapshots.

For all $n = 0, \dots, N_T$, for all $i = 1, \dots, N$, and for all $\mu_k \in \mathcal{G}_{train}$, we define the *coarse coefficients* as

$$A_{k,i}^n = \int_{\Omega} \widetilde{u}_H^n(\mu_k) \cdot \Phi_i^h \, d\mathbf{x}, \quad (15)$$

and the *fine coefficients* as

$$B_{k,i}^n = \int_{\Omega} u_h^n(\mu_k) \cdot \Phi_i^h \, d\mathbf{x}. \quad (16)$$

Then, we compute the vectors

$$\mathbf{R}_{u,i}^n = ((\mathbf{A}^n)^T \mathbf{A}^n + \delta \mathbf{I}_N)^{-1} (\mathbf{A}^n)^T \mathbf{B}_i^n, \quad i = 1, \dots, N, \quad (17)$$

where \mathbf{I}_N refers to the identity matrix and δ is a regularization parameter.

Remark 2.4. Note that since every time step has its own rectification matrix, the matrix \mathbf{A}^n is a “flat” rectangular matrix ($N_{train} \leq N$), and thus the parameter δ is required for the inversion of $(\mathbf{A}^n)^T \mathbf{A}^n$.

We also remark that with the rectification post-treatment, the standard greedy algorithm 1 may leads to more accurate approximations compared to the POD-greedy algorithm because the coefficients of the matrix \mathbf{R} are directly derived from the snapshots.

- “Online step”

The online part of the algorithm is much faster than a HF evaluation.

4. For a new parameter $\mu \in \mathcal{G}$ we are interested in, we solve the problem (11) on the coarse mesh \mathcal{T}_H at each time step $m = 0, \dots, M_T$.
5. We quadratically interpolate in time the coarse solution on the fine time grid with (12). This interpolation is denoted $\widetilde{u}_H^n(\mu)$, with $n = 0, \dots, N_T$.
6. Then, we linearly interpolate in space $\widetilde{u}_H^n(\mu)$ on the fine mesh in order to compute the L^2 -inner product with the RB functions. Finally, the approximation used in the two-grid method is

$$\text{For } n = 0, \dots, N_T, \quad u_{Hh}^{N,n}(\mu) := \sum_{i=1}^N (\widetilde{u}_H^n(\mu), \Phi_i^h) \Phi_i^h, \quad (18)$$

and with the rectification post-treatment step, it becomes

$$\mathbf{R}_u^n[u_{Hh}^N](\mu) := \sum_{i,j=1}^N R_{u,ij}^n (\widetilde{u}_H^n(\mu), \Phi_j^h) \Phi_i^h, \quad (19)$$

where $(\mathbf{R}_u^n)_{ij} = R_{u,ij}^n$ is the rectification matrix at time t^n , given by (17).

In [20], we have proven the following estimate on the heat equation

$$\text{for } n = 0, \dots, N_T, \quad \left\| u(t^n)(\mu) - u_{Hh}^{N,n}(\mu) \right\|_{H^1(\Omega)} \leq \varepsilon(N) + C_1(\mu)h + C_2(N)H^2 + C_3(\mu)\Delta t_F + C_4(N)\Delta t_G^2, \quad (20)$$

where C_1, C_2, C_3 and C_4 are constants independent of h and H , Δt_F and Δt_G . The term $\varepsilon(N)$ depends on a proper choice of the RB space as a surrogate for the best approximation space associated to the Kolmogorov N -width. It decreases when N increases and it is linked to the error between the fine solution and its projection on the reduced space X_h^N , given by

$$\left\| u_h^n(\mu) - \sum_{i=1}^N (u_h^n(\mu), \Phi_i^h) \Phi_i^h \right\|_{H^1(\Omega)}. \quad (21)$$

On the other hand, the constants $C_2(N)$ and $C_4(N)$ in (20) increase with N . Thus, a trade-off needs to be done between increasing N to obtain a more accurate manifold, and keeping these constants as low as possible.

If H is such as $H^2 \sim h$ and $\Delta t_G^2 \sim \Delta t_F$ with $C_2(N)$ and $C_4(N)$ not too large, the estimate (20) entails an error estimate in $\varepsilon(N) + \mathcal{O}(h + \Delta t_F)$. Therefore, if $\varepsilon(N)$ is small enough, we recover an optimal error estimate in $L^\infty(0, T; H^1(\Omega))$. Our aim is to extend this error estimate (20) to the context of sensitivity analysis. Before presenting the new NIRB two-grid strategies, we first recall the sensitivities problems on the heat equation in the next section.

2.3 Sensitivity analysis: The direct problem.

In this section, we recall the sensitivity systems (continuous and discretized versions) for P parameters of interest. Then, with the direct formulation, we prove several numerical results on the model problem which are used for the proof of the NIRB error estimate. To not make the notations too cumbersome in the proofs, we consider $A(\mu) = \mu I_d$, with $\mu \in \mathbb{R}_*^+$ for the analysis theorems and we drop the μ -dependency notations for u and u_0 .

2.3.1 The continuous setting.

In this setting, we consider P parameters of interest, denoted $\mu_p = 1, \dots, \mu_P$, and we aim at approximating the exact derivatives, also known as the *sensitivities*

$$\Psi_p(t, \mathbf{x}; \mu) := \frac{\partial u}{\partial \mu_p}(t, \mathbf{x}; \mu), \quad \text{in } [0, T] \times \Omega. \quad (22)$$

To do so, with the direct formulation, we solve P new systems, which can directly be obtained by differentiating the initial problem with respect to μ_p . The continuous initial problem (5) may be rewritten

$$\begin{cases} \text{Find } u(t) \in V \text{ for } t \in [0, T] \text{ such that} \\ (u_t(t), v) = F(u(t), v; \mu) := -a(u(t), v; \mu) + (f(t), v), \quad \forall v \in V, \quad t > 0, \\ u(\cdot, 0; \mu) = u^0(\cdot; \mu), \end{cases}$$

where the bilinear form a is defined by (6). Using the chain rule and since the time and the parameter derivatives can commute,

$$(\Psi_{p,t}(t), v) = \frac{\partial F}{\partial u}(u(t), v; \mu) \cdot \Psi_p(t) + \frac{\partial F}{\partial \mu}(u(t), v).$$

We therefore obtain the following problem

$$\begin{cases} \text{Find } \Psi_p(t) \in V \text{ for } t \in [0, T] \text{ such that} \\ (\Psi_{p,t}(t), v) + a(\Psi_p(t), v; \mu) = -(\frac{\partial A}{\partial \mu_p}(\mu) \nabla u(t), \nabla v), \text{ for } v \in V, \text{ for } t > 0, \\ \Psi_p^0(\mu) = \frac{\partial u^0}{\partial \mu_p}(\mathbf{x}; \mu), \end{cases} \quad (23)$$

which is well-posed since $u \in L^2(0, T; H_0^1(\Omega))$, and under the assumptions (4), the so-called “parabolic regularity estimate” implies that $u \in L^2(0, T; H^2(\Omega)) \cap L^\infty(0, T; H_0^1(\Omega))$ [15, 51].

2.3.2 The spatially semi-discretized version.

To derive the NIRB approximation, as previously for the state solution, we discretize in space and in time the sensitivity problems (23).

The corresponding spatially semi-discretized formulation on \mathcal{T}_h (similarly on \mathcal{T}_H) reads

$$\begin{cases} \text{Find } \Psi_{p,h}(t) \in V_h \text{ for } t \in [0, \dots, T] \text{ such that} \\ (\Psi_{p,h,t}(t), v_h) + a(\Psi_{p,h}(t), v_h; \mu) = -(\frac{\partial A}{\partial \mu_p}(\mu) \nabla u_h(t; \mu), \nabla v_h), \text{ for } v_h \in V_h, \text{ for } t \in]0, T], \\ \Psi_{p,h}^0(\cdot; \mu) = P_h^1(\Psi_p^0)(\cdot; \mu), \end{cases} \quad (24)$$

where P_h^1 is the Ritz projection operator given by (7). Before proceeding with the proof of Theorem (4.1), we need several theoretical results that can be deduced from [51], but require some precisions. Indeed, first, in [51], the estimates are proven on the heat equation with a non-varying diffusion coefficient. Secondly, the right-hand side function f vanishes when seeking the error estimates, whereas in our case, the right-hand side function depends on u and necessitates precised estimates.

On the semi-discretized formulation, the following estimate holds.

Theorem 2.5. *Let Ω be a convex polyhedron. Let $A(\mu) = \mu I_d$, with $\mu \in \mathbb{R}_*^+$. Consider $u \in H^1(0, T; H^2(\Omega))$ be the solution of (3) with $u^0 \in H^2(\Omega)$ and u_h be the semi-discretized variational form (8). Let Ψ and Ψ_h be the corresponding sensitivities, respectively given by (23) and (24). Then*

$$\forall t \in [0, T], \|\Psi_h(t) - \Psi(t)\|_{L^2(\Omega)} \leq Ch^2 \left[\|\Psi^0\|_{H^2(\Omega)} + \int_0^T \|\Psi_t\|_{H^2(\Omega)} ds \right] + C(\mu)h^2 \left[\int_0^T \|u_t\|_{H^2(\Omega)}^2 ds \right]^{1/2}.$$

Proof. As in [51], we first decompose the error with two components θ and ρ such that

$$\begin{aligned} \forall t \in [0, T], e(t) &:= \Psi_h(t) - \Psi(t) = (\Psi_h(t) - P_h^1 \Psi(t)) + (P_h^1 \Psi(t) - \Psi(t)), \\ &= \theta(t) + \rho(t). \end{aligned} \quad (25)$$

- For the estimate on $\rho(t)$, a classical FEM estimate [51, 5] is

$$\|P_h^1 v - v\|_{L^2(\Omega)} + h \|\nabla(P_h^1 v - v)\|_{L^2(\Omega)} \leq Ch^2 \|v\|_{H^2(\Omega)}, \quad \forall v \in H^2 \cap H_0^1, \quad (26)$$

which leads to

$$\begin{aligned} \|\rho(t)\|_{L^2(\Omega)} &\leq Ch^2 \|\Psi(t)\|_{H^2(\Omega)}, \quad \forall t \in [0, T], \\ &\leq Ch^2 \left[\|\Psi^0\|_{H^2(\Omega)} + \int_0^T \|\Psi_t\|_{H^2(\Omega)} ds \right], \quad \forall t \in [0, T]. \end{aligned} \quad (27)$$

- For the estimate on $\theta(t)$, let us consider $v \in V_h$,

$$\forall t \in]0, T], (\theta_t(t), v) + \mu(\nabla\theta(t), \nabla v) = (\Psi_{h,t}(t), v) + \mu(\nabla\Psi_h(t), \nabla v) - (P_h^1\Psi_t(t), v) - \mu(\nabla P_h^1\Psi(t), \nabla v).$$

Since $v \in H_0^1$, by definition of P_h^1 (7), the semi-discretized weak formulations (24) implies

$$\begin{aligned} (\theta_t(t), v) + \mu(\nabla\theta(t), \nabla v) &= -(\nabla u_h(t), \nabla v) - (P_h^1\Psi_t(t), v) - \mu(\nabla P_h^1\Psi(t), \nabla v), \\ &= -(\nabla u_h(t), \nabla v) - (P_h^1\Psi_t(t), v) - \mu(\nabla\Psi(t), \nabla v). \end{aligned}$$

Thanks to the continuous weak formulation (23), and since the operator P_h^1 and the time derivative commute, it can be rewritten

$$\begin{aligned} (\theta_t(t), v) + \mu(\nabla\theta(t), \nabla v) &= (\nabla u(t) - \nabla u_h(t), \nabla v) + (\Psi_t(t) - (P_h^1\Psi)_t(t), v), \\ &= (\nabla u(t) - \nabla u_h(t), \nabla v) - (\rho_t(t), v). \end{aligned}$$

Choosing $v = \theta(t)$, it yields

$$(\theta_t(t), \theta(t)) + \mu\|\nabla\theta(t)\|_{L^2(\Omega)}^2 = (\nabla u(t) - \nabla u_h(t), \nabla\theta(t)) - (\rho_t(t), \theta(t)),$$

and using the continuous and semi-discretized weak formulations on the state variable $u(t)$ ((5) and (8) respectively), we obtain

$$(\theta_t(t), \theta(t)) + \mu\|\nabla\theta(t)\|_{L^2(\Omega)}^2 = \frac{1}{\mu}(u_{h,t}(t) - u_t(t), \theta(t)) - (\rho_t(t), \theta(t)), \quad (28)$$

where the first term of the right-hand side is a new contribution (compared to the proof of Theorem 1.2 [51]). Since

$$(\theta_t(t), \theta(t)) = \frac{1}{2} \frac{d}{dt} (\|\theta(t)\|_{L^2(\Omega)}^2) = \|\theta(t)\|_{L^2(\Omega)} \frac{d}{dt} \|\theta(t)\|_{L^2(\Omega)}, \quad (29)$$

and, since the second term in (28) is positive, it becomes with Cauchy-Schwarz inequality (the case where $\theta(t) = 0$ for some t may easily be handled)

$$\frac{d}{dt} \|\theta(t)\|_{L^2(\Omega)} \leq \frac{1}{\mu} \|u_{h,t}(t) - u_t(t)\|_{L^2(\Omega)} + \|\rho_t(t)\|_{L^2(\Omega)}.$$

Integrating over time, it follows that

$$\|\theta(t)\|_{L^2(\Omega)} \leq \underbrace{\|\theta(0)\|_{L^2(\Omega)}}_{T_1} + \underbrace{\frac{1}{\mu} \int_0^T \|u_{h,t} - u_t\|_{L^2(\Omega)} \, ds}_{T_2} + \underbrace{\int_0^T \|\rho_t\|_{L^2(\Omega)} \, ds}_{T_3}. \quad (30)$$

- From the initial conditions, since $u_h^0 = P_h^1 u^0$, $T_1 = 0$. Note that other optimal order choices of discretized initial conditions (such as the L^2 orthogonal projection onto V_h) lead to an estimate in $Ch^2 \|\Psi^0\|_{H^2(\Omega)}$ for T_1 .
- To estimate T_2 , in analogy with θ and ρ , let us introduce θ_u and ρ_u , such that

$$\begin{aligned} \forall t \in [0, T], u_h(t) - u(t) &= (u_h(t) - P_h^1 u(t)) + (P_h^1 u(t) - u(t)), \\ &= \theta_u(t) + \rho_u(t). \end{aligned} \quad (31)$$

We remark that the term T_2 can also be written

$$T_2 = \frac{1}{\mu} \int_0^T \|\theta_{u,t} + \rho_{u,t}\|_{L^2(\Omega)} \, ds \leq \frac{1}{\mu} \int_0^T \|\theta_{u,t}\|_{L^2(\Omega)} + \|\rho_{u,t}\|_{L^2(\Omega)} \, ds.$$

Then, by Cauchy-Schwarz inequality,

$$T_2 \leq \frac{\sqrt{T}}{\mu} \left(\left[\int_0^T \|\theta_{u,t}\|_{L^2(\Omega)}^2 \, ds \right]^{1/2} + \left[\int_0^T \|\rho_{u,t}\|_{L^2(\Omega)}^2 \, ds \right]^{1/2} \right), \quad (32)$$

We can bound $\int_0^T \|\theta_{u,t}\|_{L^2(\Omega)}^2$, using the variational formulations (5) and (8). We first write for $t \in]0, T]$:

$$\begin{aligned} (\theta_{u,t}(t), v) + \mu(\nabla \theta_u(t), \nabla v) &= (u_{h,t}(t), v) + \mu(\nabla u_h(t), \nabla v) - (P_h^1 u_t(t), v) - \mu(\nabla P_h^1 u(t), \nabla v), \\ &= (f(t), v) - (P_h^1 u_t(t), v) - \mu(\nabla u(t), \nabla v), \\ &= -(\rho_{u,t}(t), v). \end{aligned}$$

Formally by using $v = \theta_{u,t}(t)$ and (29), it entails

$$\|\theta_{u,t}(t)\|_{L^2(\Omega)}^2 + \frac{\mu}{2} \frac{d}{dt} \|\nabla \theta_u(t)\|_{L^2(\Omega)}^2 = -(\rho_{u,t}(t), \theta_{u,t}(t)),$$

such that (with Young's inequality)

$$\|\theta_{u,t}(t)\|_{L^2(\Omega)}^2 + \mu \frac{d}{dt} \|\nabla \theta_u(t)\|_{L^2(\Omega)}^2 \leq \|\rho_{u,t}(t)\|_{L^2(\Omega)}^2.$$

Integrating over time, we obtain

$$\int_0^T \|\theta_{u,t}\|_{L^2(\Omega)}^2 \, ds + \mu \|\nabla \theta_u(t)\|_{L^2(\Omega)}^2 \leq \mu \|\nabla \theta_u(0)\|_{L^2(\Omega)}^2 + \int_0^T \|\rho_{u,t}\|_{L^2(\Omega)}^2 \, ds,$$

and since the second term is always positive and that we have chosen $u_h^0 = P_h^1 u^0$, it yields

$$\int_0^T \|\theta_{u,t}\|_{L^2(\Omega)}^2 \leq \int_0^T \|\rho_{u,t}\|_{L^2(\Omega)}^2. \quad (33)$$

Remark 2.6. Note that with another choice of discretized initial solution, we would have

$$\|\nabla \theta_u(0)\|_{L^2(\Omega)}^2 \leq \|\nabla u_h^0 - \nabla u^0\|_{L^2(\Omega)}^2 + Ch^2 \|u^0\|_{H^2(\Omega)}^2,$$

which would have lead to an estimate in $\mathcal{O}(h)$ on the $L^2(\Omega)$ error estimate of $\Psi(t)$. In practice, this is not an issue since the effect of the initial data exponentially decreases [51].

Therefore, from (32), we obtain

$$T_2 \leq \frac{2\sqrt{T}}{\mu} \left[\int_0^T \|\rho_{u,t}\|_{L^2(\Omega)}^2 \, ds \right]^{1/2}. \quad (34)$$

By definition of P_h^1 (7), we have

$$\|\rho_{u,t}(t)\|_{L^2(\Omega)} = \|P_h^1 u_t(t) - u_t(t)\|_{L^2(\Omega)} \leq Ch^2 \|u_t(t)\|_{H^2(\Omega)}, \quad (35)$$

and thus, (34) yields

$$T_2 \leq C \frac{2\sqrt{T}}{\mu} h^2 \left[\int_0^T \|u_t\|_{H^2(\Omega)}^2 \, ds \right]^{1/2}. \quad (36)$$

– Finally, for T_3 , we only need to use (35) again, but with Ψ instead of u . Therefore

$$T_3 = \int_0^T \|\rho_t\|_{L^2(\Omega)} \, ds \leq Ch^2 \int_0^T \|\Psi_t\|_{H^2(\Omega)} \, ds. \quad (37)$$

Combining (27), (30), (36), and (37) concludes the proof. \square

We can derive a similar result for the H_0^1 norm.

Theorem 2.7. Let Ω be a convex polyhedron. Let $A(\mu) = \mu I_d$, with $\mu \in \mathbb{R}_*^+$. Consider $u \in H^1(0, T; H^2(\Omega))$ be the solution of (3) with $u^0 \in H^2(\Omega)$ and u_h be the semi-discretized variational form (8). Let Ψ and Ψ_h be the corresponding sensitivities, respectively given by (23) and (24).

$\forall t \in [0, T]$,

$$\|\Psi(t) - \Psi_h(t)\|_{H^1(\Omega)} \leq Ch \left[\|\Psi^0\|_{H^2(\Omega)} + \int_0^T \|\Psi_t\|_{H^2(\Omega)} \, ds \right] + C(\mu) h^2 \left(\left[\int_0^T \|u_t\|_{H^2}^2 \, ds \right]^{1/2} + \left[\int_0^T \|\Psi_t\|_{H^2(\Omega)}^2 \, ds \right]^{1/2} \right).$$

Proof. Using the same notation as before (25), we first decompose the error with the two components θ and ρ such that

$$\forall t \in [0, T], \nabla \Psi_h(t) - \nabla \Psi(t) = \nabla \theta(t) + \nabla \rho(t). \quad (38)$$

- For the estimate on $\rho(t)$, we use (26) to obtain

$$\|\nabla \rho(t)\|_{L^2(\Omega)} \leq Ch \|\Psi(t)\|_{H^2(\Omega)}, \quad \forall t \in [0, T],$$

which leads to

$$\|\nabla \rho(t)\|_{L^2(\Omega)} \leq Ch \left[\|\Psi^0\|_{H^2(\Omega)} + \int_0^T \|\Psi_t\|_{H^2(\Omega)} \, ds \right], \quad \forall t \in [0, T]. \quad (39)$$

- For the estimate on $\theta(t)$, let us consider $v \in V_h$. As in the previous proof, $\forall t \in [0, T]$, we write

$$(\theta_t(t), v) + \mu(\nabla \theta(t), \nabla v) = (\Psi_{h,t}(t), v) + \mu(\nabla \Psi_h(t), \nabla v) - (P_h^1 \Psi_t(t), v) - \mu(\nabla P_h^1 \Psi(t), \nabla v).$$

Instead of replacing v by $\theta(t)$ as in the L^2 estimate, here we formally replace v by $\theta_t(t)$, thus

$$\forall t \in]0, T], \quad \|\theta_t(t)\|_{L^2(\Omega)}^2 + \mu(\nabla \theta(t), \nabla \theta_t(t)) = (\nabla u(t) - \nabla u_h(t), \nabla \theta_t(t)) - (\rho_t(t), \theta_t(t)).$$

Thanks to the variational formulations on the state solution u ((5) and (8) respectively)

$$\|\theta_t(t)\|_{L^2(\Omega)}^2 + \mu(\nabla \theta(t), \nabla \theta_t(t)) = \left(\frac{1}{\mu} (u_{h,t}(t) - u_t(t)), \theta_t(t) \right) - (\rho_t(t), \theta_t(t)),$$

and thus (with Young's inequality),

$$\begin{aligned} \|\theta_t(t)\|_{L^2(\Omega)}^2 + \mu(\nabla \theta(t), \nabla \theta_t(t)) &\leq \frac{1}{2} \left\| \frac{1}{\mu} (u_{h,t}(t) - u_t(t)) \right\|_{L^2(\Omega)}^2 + \frac{1}{2} \|\theta_t(t)\|_{L^2(\Omega)}^2 + \frac{1}{2} \|\rho_t(t)\|_{L^2(\Omega)}^2 + \frac{1}{2} \|\theta_t(t)\|_{L^2(\Omega)}^2, \\ &\leq \frac{1}{2\mu^2} \|u_{h,t}(t) - u_t(t)\|_{L^2(\Omega)}^2 + \frac{1}{2} \|\rho_t(t)\|_{L^2(\Omega)}^2 + \|\theta_t(t)\|_{L^2(\Omega)}^2. \end{aligned}$$

Thus,

$$\mu(\nabla \theta(t), \nabla \theta_t(t)) \leq \frac{1}{2\mu^2} \|u_{h,t}(t) - u_t(t)\|_{L^2(\Omega)}^2 + \frac{1}{2} \|\rho_t(t)\|_{L^2(\Omega)}^2, \quad (40)$$

and by (29), we have

$$\frac{d}{dt} \|\nabla \theta(t)\|_{L^2(\Omega)}^2 \leq \frac{1}{\mu^3} \|u_{h,t}(t) - u_t(t)\|_{L^2(\Omega)}^2 + \frac{1}{\mu} \|\rho_t(t)\|_{L^2(\Omega)}^2.$$

Integrating over time, it entails

$$\|\nabla \theta(t)\|_{L^2(\Omega)}^2 \leq \underbrace{\|\nabla \theta(0)\|_{L^2(\Omega)}^2}_{T'_1} + \underbrace{\frac{1}{\mu^3} \int_0^T \|u_{h,t} - u_t\|_{L^2(\Omega)}^2 \, ds}_{T'_2} + \underbrace{\frac{1}{\mu} \int_0^T \|\rho_t\|_{L^2(\Omega)}^2 \, ds}_{T'_3}. \quad (41)$$

– From the initial conditions, $T'_1 = 0$.

– We can also write T'_2 as

$$T'_2 = \frac{1}{\mu^3} \int_0^T \|\theta_{u,t} + \rho_{u,t}\|_{L^2(\Omega)}^2 \, ds.$$

Therefore using (33),

$$T'_2 \leq \frac{2}{\mu^3} \int_0^T \|\theta_{u,t}\|_{L^2(\Omega)}^2 + \|\rho_{u,t}\|_{L^2(\Omega)}^2 \, ds \leq \frac{4}{\mu^3} \int_0^T \|\rho_{u,t}\|_{L^2(\Omega)}^2 \, ds \leq \frac{Ch^4}{\mu^3} \int_0^T \|u_t\|_{H^2(\Omega)}^2 \, ds. \quad (42)$$

– Similarly,

$$T'_3 \leq \frac{Ch^4}{\mu} \int_0^T \|\Psi_t\|_{H^2(\Omega)}^2 \, ds. \quad (43)$$

Hence, combining (38) with (39), (41), (42) and (43) concludes the proof. \square

2.3.3 The fully-discretized versions.

From (24), we can derive the fully-discretized systems for the fine and coarse grids.

The direct sensitivity problems with respect to the parameter μ_p on the fine mesh \mathcal{T}_h with an Euler scheme read

$$\left\{ \begin{array}{l} \text{Find } \Psi_{p,h}^n \in V_h \text{ for } n \in \{0, \dots, N_T\} \text{ such that} \\ (\bar{\partial} \Psi_{p,h}^n, v_h) + a(\Psi_{p,h}^n, v_h; \mu) = -(\frac{\partial A}{\partial \mu_p}(\mu) \nabla u_h^n(\mu), \nabla v_h), \text{ for } v_h \in V_h, \text{ for } n = \{1, \dots, N_T\}, \\ \Psi_{p,h}^0(\cdot; \mu) = P_h^1 \Psi_p^0(\cdot; \mu), \end{array} \right. \quad (44)$$

where, as before, the time derivative in the variational form of the problem (23) has been replaced by a backward difference quotient, $\bar{\partial} \Psi_h^n = \frac{\Psi_h^n - \Psi_h^{n-1}}{\Delta t_F}$.

With the fully-discretized version (44), the following estimate holds.

Theorem 2.8. *Let Ω be a convex polyhedron. Let $A(\mu) = \mu I_d$, with $\mu \in \mathbb{R}_*^+$.*

Consider $u \in H^1(0, T; H^2(\Omega)) \cap H^2(0, T; L^2(\Omega))$ be the solution of (3) with $u^0 \in H^2(\Omega)$ and u_h^n be the fully-discretized variational form (10). Let Ψ and Ψ_h^n be the corresponding sensitivities, respectively given by (23) and (44). Then

$$\begin{aligned} \forall n = 0, \dots, N_T, \|\Psi_h^n - \Psi(t)\|_{L^2(\Omega)} &\leq Ch^2 \|\Psi^0\|_{H^2(\Omega)} + h^2 \left(C \int_0^{t^n} \|\Psi_t\|_{H^2(\Omega)} ds + C(\mu) \left[\int_0^{t^n} \|u_t\|_{H^2(\Omega)}^2 ds \right]^{1/2} \right) \\ &\quad + \Delta t_F \left(C \int_0^{t^n} \|\Psi_{tt}\|_{L^2(\Omega)} ds + C(\mu) \left[\int_0^{t^n} \|u_{tt}\|_{L^2(\Omega)}^2 ds \right]^{1/2} \right). \end{aligned}$$

Proof. Now, we define θ^n and ρ^n on the discretized time grid $(t^n)_{n=0, \dots, N_T}$.

$$\begin{aligned} \forall n = 0, \dots, N_T, e^n := \Psi_h^n - \Psi(t^n) &= (\Psi_h^n - P_h^1 \Psi(t^n)) + (P_h^1 \Psi(t^n) - \Psi(t^n)), \\ &= \theta^n + \rho^n. \end{aligned} \quad (45)$$

- In analogy with (26) the estimate on ρ^n is

$$\|\rho^n\|_{L^2(\Omega)} \leq Ch^2 \|\Psi(t^n)\|_{H^2(\Omega)} \leq Ch^2 \left[\|\Psi^0\|_{H^2(\Omega)} + \int_0^{t^n} \|\Psi_t\|_{H^2(\Omega)} ds \right], \quad \forall n \in \{0, \dots, N_T\}. \quad (46)$$

- For θ^n , the equation (28) becomes

$$\begin{aligned} (\bar{\partial} \theta^n, \theta^n) + \mu \|\nabla \theta^n\|_{L^2(\Omega)}^2 &= \frac{1}{\mu} (\bar{\partial} u_h^n - u_t(t^n), \theta^n) - (w_1^n + w_2^n, \theta^n), \\ &= \frac{1}{\mu} (\bar{\partial} u_h^n - u_t(t^n), \theta^n) - (w^n, \theta^n), \end{aligned} \quad (47)$$

where w_1^n and w_2^n are defined by

$$w_1^n := (P_h^1 - I) \bar{\partial} \Psi(t^n), \quad w_2^n := \bar{\partial} \Psi(t^n) - \Psi_t(t^n), \quad \text{and} \quad w^n := w_1^n + w_2^n. \quad (48)$$

By definition of $\bar{\partial}$ and by Cauchy-Schwarz inequality (and since the second term of the left-hand side of (47) is always positive),

$$\|\theta^n\|_{L^2(\Omega)}^2 \leq \left(\|\theta^{n-1}\|_{L^2(\Omega)} + \Delta t_F \left[\frac{1}{\mu} \|\bar{\partial} u_h^n - u_t(t^n)\|_{L^2(\Omega)} + \|w^n\|_{L^2(\Omega)} \right] \right) \|\theta^n\|_{L^2(\Omega)},$$

and by repeated application, and since $\|\theta^0\|_{L^2(\Omega)} = 0$ (again, the case where some θ^n are equal to 0 can be easily handled), it entails

$$\|\theta^n\|_{L^2(\Omega)} \leq \underbrace{\Delta t_F \sum_{j=1}^n \frac{1}{\mu} \|\bar{\partial} u_h^j - u_t(t^j)\|_{L^2(\Omega)}}_{T_{2,n}} + \underbrace{\Delta t_F \sum_{j=1}^n \|w^j\|_{L^2(\Omega)}}_{T_{3,n}}, \quad (49)$$

– We first decompose $T_{2,n}$ in two contributions

$$\frac{\Delta t_F}{\mu} \sum_{j=1}^n \left\| \bar{\partial} u_h^j - u_t(t^j) \right\|_{L^2(\Omega)} \leq \frac{\Delta t_F}{\mu} \sum_{j=1}^n \left(\left\| \bar{\partial} \theta_u^j \right\|_{L^2(\Omega)} + \left\| w_u^j \right\|_{L^2(\Omega)} \right),$$

where

$$w_u^j := w_{1,u}^j + w_{2,u}^j \text{ with } w_{1,u}^j := (P_h^1 - I) \bar{\partial} u(t^j), \text{ and } w_{2,u}^j := \bar{\partial} u(t^j) - u_t(t^j). \quad (50)$$

Then by using Cauchy-Schwarz inequality (as in the semi-discretized case (32)),

$$\frac{\Delta t_F}{\mu} \sum_{j=1}^n \left\| \bar{\partial} u_h^j - u_t(t^j) \right\|_{L^2(\Omega)} \leq \frac{\sqrt{t^n}}{\mu} \left[\underbrace{\left(\sum_{j=1}^n \Delta t_F \left\| \bar{\partial} \theta_u^j \right\|_{L^2(\Omega)}^2 \right)^{1/2}}_{T_\theta} + \underbrace{\left(\sum_{j=1}^n \Delta t_F \left\| w_u^j \right\|_{L^2(\Omega)}^2 \right)^{1/2}}_{T_w} \right]. \quad (51)$$

* Let us begin by the estimate on T_θ . On the state solution u , by choosing $v = \bar{\partial} \theta_u^n$, from (10) (the operator $\bar{\partial}$ and the spatial derivative can commute), we have

$$\left\| \bar{\partial} \theta_u^n \right\|_{L^2(\Omega)}^2 + \mu (\nabla \theta_u^n, \bar{\partial} \nabla \theta_u^n) = - (w_u^n, \bar{\partial} \theta_u^n), \quad (52)$$

where θ_u^n is the discrete version of (31). By definition of $\bar{\partial}$ (and with Young's inequality),

$$\left\| \bar{\partial} \theta_u^n \right\|_{L^2(\Omega)}^2 + \frac{\mu}{\Delta t_F} \left\| \nabla \theta_u^n \right\|_{L^2(\Omega)}^2 \leq \frac{\mu}{2 \Delta t_F} \left(\left\| \nabla \theta_u^n \right\|_{L^2(\Omega)}^2 + \left\| \nabla \theta_u^{n-1} \right\|_{L^2(\Omega)}^2 \right) + \frac{1}{2} \left(\left\| w_u^n \right\|_{L^2(\Omega)}^2 + \left\| \bar{\partial} \theta_u^n \right\|_{L^2(\Omega)}^2 \right),$$

which entails

$$\left\| \bar{\partial} \theta_u^n \right\|_{L^2(\Omega)}^2 \leq \frac{\mu}{\Delta t_F} \left\| \nabla \theta_u^{n-1} \right\|_{L^2(\Omega)}^2 - \frac{\mu}{\Delta t_F} \left\| \nabla \theta_u^n \right\|_{L^2(\Omega)}^2 + \left\| w_u^n \right\|_{L^2(\Omega)}^2, \quad \forall n = 1, \dots, N_T. \quad (53)$$

Summing over the time steps, we get

$$\sum_{j=1}^n \left\| \bar{\partial} \theta_u^j \right\|_{L^2(\Omega)}^2 \leq \left| \sum_{j=1}^n \frac{\mu}{\Delta t_F} \left[\left\| \nabla \theta_u^{j-1} \right\|_{L^2(\Omega)}^2 - \left\| \nabla \theta_u^j \right\|_{L^2(\Omega)}^2 \right] + \left\| w_u^j \right\|_{L^2(\Omega)}^2 \right|,$$

and we obtain

$$\sum_{j=1}^n \left\| \bar{\partial} \theta_u^j \right\|_{L^2(\Omega)}^2 \leq \left| \frac{\mu}{\Delta t_F} \left(\left\| \nabla \theta_u^0 \right\|_{L^2(\Omega)}^2 - \left\| \nabla \theta_u^n \right\|_{L^2(\Omega)}^2 \right) \right| + \sum_{j=1}^n \left\| w_u^j \right\|_{L^2(\Omega)}^2.$$

From the initial condition, $\theta_u^0 = 0$,

$$\sum_{j=1}^n \left\| \bar{\partial} \theta_u^j \right\|_{L^2(\Omega)}^2 \leq \frac{\mu}{\Delta t_F} \left\| \nabla \theta_u^n \right\|_{L^2(\Omega)}^2 + \sum_{j=1}^n \left\| w_u^j \right\|_{L^2(\Omega)}^2. \quad (54)$$

From (53) and by repeated application, we find for the first right-hand side term that

$$\left\| \nabla \theta_u^n \right\|_{L^2(\Omega)}^2 \leq \frac{\Delta t_F}{\mu} \sum_{j=1}^n \left\| w_u^j \right\|_{L^2(\Omega)}^2,$$

which gives for (54), multiplying by Δt_F to recover T_θ ,

$$\sum_{j=1}^n \Delta t_F \left\| \bar{\partial} \theta_u^j \right\|_{L^2(\Omega)}^2 \leq 2 \sum_{j=1}^n \Delta t_F \left\| w_u^j \right\|_{L^2(\Omega)}^2. \quad (55)$$

Now, going back to (51), we obtain

$$\frac{\Delta t_F}{\mu} \sum_{j=1}^n \left\| \bar{\partial} u_h^j - u_t(t^j) \right\|_{L^2(\Omega)} \leq \frac{C}{\mu} \underbrace{\left(\sum_{j=1}^n \Delta t_F \left\| w_u^j \right\|_{L^2(\Omega)}^2 \right)^{1/2}}_{T_w} \leq \frac{C}{\mu} \left(\sum_{j=1}^n \Delta t_F \left[\left\| w_{1,u}^j \right\|_{L^2(\Omega)}^2 + \left\| w_{2,u}^j \right\|_{L^2(\Omega)}^2 \right] \right)^{1/2}. \quad (56)$$

* It remains to estimate T_w .

· Let us first consider the construction for $w_{1,u}$

$$w_{1,u}^j = (P_h^1 - I)\bar{\partial}u(t^j) = \frac{1}{\Delta t_F}(P_h^1 - I) \int_{t^{j-1}}^{t^j} u_t \, ds = \frac{1}{\Delta t_F} \int_{t^{j-1}}^{t^j} (P_h^1 - I)u_t \, ds ,$$

since P_h^1 and the time integral commute. Thus, from Cauchy-Schwarz inequality,

$$\begin{aligned} \Delta t_F \sum_{j=1}^n \|w_{1,u}^j\|_{L^2(\Omega)}^2 &\leq \Delta t_F \sum_{j=1}^n \int_{\Omega} \left[\frac{1}{\Delta t_F^2} \int_{t^{j-1}}^{t^j} ((P_h^1 - I)u_t)^2 \, ds \, \Delta t_F \right] \\ &\leq \sum_{j=1}^n \int_{t^{j-1}}^{t^j} \|(P_h^1 - I)u_t\|_{L^2(\Omega)}^2 \, ds , \\ &\leq Ch^4 \sum_{j=1}^n \int_{t^{j-1}}^{t^j} \|u_t\|_{H^2(\Omega)}^2 \, ds , \text{ by definition of } P_h^1, \\ &\leq Ch^4 \int_0^{t^n} \|u_t\|_{H^2(\Omega)}^2 \, ds. \end{aligned} \quad (57)$$

· To estimate the L^2 norm of $w_{2,u}$, we write

$$w_{2,u}^j = \frac{1}{\Delta t_F}(u(t^j) - u(t^{j-1})) - u_t(t^j) = -\frac{1}{\Delta t_F} \int_{t^{j-1}}^{t^j} (s - t^{j-1})u_{tt}(s) \, ds,$$

such that we end up with

$$\Delta t_F \sum_{j=1}^n \|w_{2,u}^j\|_{L^2(\Omega)}^2 \leq \sum_{j=1}^n \left\| \int_{t^{j-1}}^{t^j} (s - t^{j-1})u_{tt}(s) \, ds \right\|_{L^2(\Omega)}^2 \leq \Delta t_F^2 \int_0^{t^n} \|u_{tt}\|_{L^2(\Omega)}^2 \, ds, \quad (58)$$

– We still have to find a bound for $T_{3,n}$, defined in (49).

* For the estimates on w_1^j ,

$$w_1^j = \frac{1}{\Delta t_F} \int_{t^{j-1}}^{t^j} (P_h^1 - I)\Psi_t \, ds ,$$

and thus,

$$\Delta t_F \sum_{j=1}^n \|w_1^j\|_{L^2(\Omega)} \leq Ch^2 \int_0^{t^n} \|\Psi_t\|_{H^2(\Omega)} \, ds .$$

* For w_2^j , we have

$$\Delta t_F w_2^j = \Psi(t^j) - \Psi(t^{j-1}) - \Delta t_F \Psi_t(t^j) = - \int_{t^{j-1}}^{t^j} (s - t^{j-1})\Psi_{tt}(s) \, ds ,$$

and therefore

$$\Delta t_F \sum_{j=1}^n \|w_2^j\|_{L^2(\Omega)} \leq \sum_{j=1}^n \left\| \int_{t^{j-1}}^{t^j} (s - t^{j-1})\Psi_{tt}(s) \, ds \right\|_{L^2(\Omega)} \leq \Delta t_F \int_0^{t^n} \|\Psi_{tt}\|_{L^2(\Omega)} \, ds .$$

Altogether,

$$T_{3,n} \leq Ch^2 \int_0^{t^n} \|\Psi_t\|_{H^2(\Omega)} \, ds + \Delta t_F \int_0^{t^n} \|\Psi_{tt}\|_{L^2(\Omega)} \, ds , \quad (59)$$

and the proof ends by using (46), (49), (56), (57), (58), and (59).

□

With the fully-discretized version (44), the following estimate holds with H^1 norm.

Theorem 2.9. Let Ω be a convex polyhedron. Let $A(\mu) = \mu I_d$, with $\mu \in \mathbb{R}_*^+$.

Consider $u \in H^1(0, T; H^2(\Omega)) \cap H^2(0, T; L^2(\Omega))$ be the solution of (3) with $u^0 \in H^2(\Omega)$ and u_h^n be the fully-discretized variational form (10). Let Ψ and Ψ_h^n be the corresponding sensitivities, respectively given by (23) and (44). Then

$$\forall n = 0, \dots, N_T, \|\nabla \Psi_h^n - \nabla \Psi(t)\|_{L^2(\Omega)} \leq h \left[C \|\Psi^0\|_{H^2(\Omega)} + C(\mu) \int_0^{t^n} \|\Psi_t\|_{H^2(\Omega)} ds + C(\mu) \left[\int_0^{t^n} \|u_t\|_{H^2(\Omega)}^2 ds \right]^{1/2} \right] \\ + C(\mu) \Delta t_F \left(\int_0^{t^n} \|\Psi_{tt}\|_{L^2(\Omega)} ds + \left[\int_0^{t^n} \|u_{tt}\|_{L^2(\Omega)}^2 ds \right]^{1/2} \right).$$

Proof. The proof combines the ideas of the two previous ones, since we seek the estimate in the H^1 norm (as in the semi-discretized problem) but with the fully-discretized version.

- In analogy with (26), the estimate on ρ^n is now given by

$$\|\nabla \rho^n\|_{L^2(\Omega)} \leq Ch \|\Psi(t^n)\|_{H^2(\Omega)} \leq Ch \left[\|\Psi^0\|_{H^2(\Omega)} + \int_0^{t^n} \|\Psi_t\|_{H^2(\Omega)} ds \right], \quad \forall n = 0, \dots, N_T. \quad (60)$$

- For θ^n , instead of choosing $v = \theta^n$ as in (47), we take $v = \bar{\partial}\theta^n$

$$\|\bar{\partial}\theta^n\|_{L^2(\Omega)}^2 + \mu(\nabla\theta^n, \nabla\bar{\partial}\theta^n) = \frac{1}{\mu}(\bar{\partial}u_h^n - u_t(t^n), \bar{\partial}\theta^n) - (w^n, \bar{\partial}\theta^n), \quad (61)$$

and we obtain (as before with the semi-discretized version (40))

$$\mu(\nabla\theta^n, \nabla\bar{\partial}\theta^n) \leq \frac{1}{2\mu^2} \|\bar{\partial}u_h^n - u_t(t^n)\|_{L^2(\Omega)}^2 + \frac{1}{2} \|w^n\|_{L^2(\Omega)}^2.$$

By definition of $\bar{\partial}$

$$\mu \|\nabla\theta^n\|_{L^2(\Omega)}^2 \leq (\sqrt{\mu}\nabla\theta^n, \sqrt{\mu}\nabla\theta^{n-1}) + \frac{\Delta t_F}{2\mu^2} \|\bar{\partial}u_h^n - u_t(t^n)\|_{L^2(\Omega)}^2 + \frac{\Delta t_F}{2} \|w^n\|_{L^2(\Omega)}^2,$$

which entails (by Young's inequality)

$$\mu \|\nabla\theta^n\|_{L^2(\Omega)}^2 \leq \mu \|\nabla\theta^{n-1}\|_{L^2(\Omega)}^2 + \frac{\Delta t_F}{\mu^2} \|\bar{\partial}u_h^n - u_t(t^n)\|_{L^2(\Omega)}^2 + \Delta t_F \|w^n\|_{L^2(\Omega)}^2,$$

and, by recursion (as in (49))

$$\mu \|\nabla\theta^n\|_{L^2(\Omega)}^2 \leq \underbrace{\frac{\Delta t_F}{\mu^2} \sum_{j=1}^n \|\bar{\partial}u_h^j - u_t(t^j)\|_{L^2(\Omega)}^2}_{T'_{2,n}} + \underbrace{\Delta t_F \sum_{j=1}^n \|w^j\|_{L^2(\Omega)}^2}_{T'_{3,n}}. \quad (62)$$

– To estimate $T'_{2,n}$, we write

$$T'_{2,n} \leq \frac{2}{\mu^2} \left[\underbrace{\sum_{j=1}^n \Delta t_F \|\bar{\partial}\theta_u^j\|_{L^2(\Omega)}^2}_{T_\theta} + \underbrace{\sum_{j=1}^n \Delta t_F \|w_u^j\|_{L^2(\Omega)}^2}_{T_w} \right],$$

and thanks to the previous estimate on T_θ (55), we find that

$$T'_{2,n} \leq \frac{6}{\mu^2} \left[\underbrace{\sum_{j=1}^n \Delta t_F \|w_u^j\|_{L^2(\Omega)}^2}_{T_w} \right],$$

which, by (57) and (58), yields

$$T'_{2,n} \leq \frac{C}{\mu^2} \left[h^4 \int_0^{t^n} \|u_t\|_{H^2(\Omega)}^2 ds + \Delta t_F^2 \int_0^{t^n} \|u_{tt}\|_{L^2(\Omega)}^2 ds \right].$$

- To find a bound for $T'_{3,n}$, we simply use (57) and (58) again but with the sensitivity function Ψ instead of u .

Combining the estimates on $T'_{2,n}$ and $T'_{3,n}$ with (62), and (60) concludes the proof. \square

With $\bar{\partial}\Psi_H^m = \frac{\Psi_H^m - \Psi_H^{m-1}}{\Delta t_G}$, on the coarse mesh \mathcal{T}_H with the Crank-Nicolson scheme, the fully-discretized system (11) yields

$$\begin{cases} \text{Find } \Psi_{p,H}^m \in V_H \text{ for } m \in \{0, \dots, M_T\} \text{ such that} \\ (\bar{\partial}\Psi_{p,H}^m, v_H) + a\left(\frac{\Psi_{p,H}^m + \Psi_{p,H}^{m-1}}{2}, v_H; \mu\right) = -\left(\frac{\partial A}{\partial \mu_p}(\mu) \frac{\nabla u_H^m(\mu) + \nabla u_H^{m-1}(\mu)}{2}, \nabla v_H\right), \text{ for } v_H \in V_H, \text{ for } m = \{1, \dots, M_T\}, \\ \Psi_{p,H}^0(\cdot; \mu) = P_H^1 \Psi_p^0(\cdot; \mu). \end{cases} \quad (63)$$

We have the following result in the L^2 norm with the Crank-Nicolson scheme on the coarse mesh \mathcal{T}_H .

Theorem 2.10. *Let Ω be a convex polyhedron. Let $A(\mu) = \mu I_d$, with $\mu \in \mathbb{R}_+^*$.*

Consider $u \in H^2(0, T; H^2(\Omega)) \cap H^3(0, T; L^2(\Omega))$ be the solution of (3) with $u^0 \in H^2(\Omega)$ and u_H^m be the fully-discretized variational form (11) (on the coarse mesh \mathcal{T}_H). Let Ψ and Ψ_H^m be the corresponding sensitivities, respectively given by (23) and (44). Then

$$\begin{aligned} \forall m = 0, \dots, M_T, \left\| \Psi_H^m - \Psi(\tilde{t}^m) \right\|_{L^2(\Omega)} &\leq CH^2 \left[\left\| \Psi^0 \right\|_{H^2(\Omega)} + \int_0^{\tilde{t}^m} \left\| \Psi_t \right\|_{H^2(\Omega)} ds + C(\mu) \left[\int_0^{\tilde{t}^m} \|u_t\|_{H^2(\Omega)}^2 ds \right]^{1/2} \right] \\ &\quad + C\Delta t_G^2 \left(\int_0^{\tilde{t}^m} \left\| \Psi_{tt} \right\|_{L^2(\Omega)} ds + \left[\int_0^{\tilde{t}^m} \left\| \Delta u_{tt} \right\|_{L^2(\Omega)}^2 ds \right]^{1/2} + C(\mu) \left[\int_0^{\tilde{t}^m} \|u_{ttt}\|_{L^2(\Omega)}^2 ds \right]^{1/2} + \int_0^{\tilde{t}^m} \left\| \Delta \Psi_{tt} \right\|_{L^2(\Omega)} ds \right). \end{aligned}$$

Proof. • For ρ^m we have the same estimate as before (46) (but with the coarse size H).

- We introduce the following notation

$$\widehat{u}_H^m = \frac{1}{2}(u_H^m + u_H^{m-1}). \quad (64)$$

Thanks to the Crank-Nicolson formulation on Ψ_H^m (63) and u_H^m (11) on the coarse mesh \mathcal{T}_H (and on the weak formulation on u (5) and by definition of P_H^1 (7)),

$$\begin{aligned} (\bar{\partial}\theta^m, v) + \mu(\nabla \widehat{\theta}^m, \nabla v) &= (\bar{\partial}\Psi_H^m, v) - (\bar{\partial}P_H^1(\Psi(\tilde{t}^m)), v) + \mu(\nabla \widehat{\Psi}_H^m, \nabla v) - \frac{\mu}{2} \left((\nabla P_H^1 \Psi(\tilde{t}^m), \nabla v) + (\nabla P_H^1 \Psi(\tilde{t}^{m-1}), \nabla v) \right), \\ &= -(\nabla \widehat{u}_H^m, \nabla v) - (\bar{\partial}P_H^1(\Psi(\tilde{t}^m)), v) - \frac{\mu}{2} \left((\nabla \Psi(\tilde{t}^m), \nabla v) + (\nabla \Psi(\tilde{t}^{m-1}), \nabla v) \right), \\ &= -(\nabla \widehat{u}_H^m, \nabla v) - \underbrace{(\bar{\partial}P_H^1(\Psi(\tilde{t}^m)), v)}_{-w_I^m} + \underbrace{(\bar{\partial}\Psi(\tilde{t}^m), v)}_{-w_{II}^m} - \underbrace{(\bar{\partial}\Psi(\tilde{t}^{m-1}), v)}_{-w_{III}^m} + \frac{\mu}{2} \left((\nabla \Psi(\tilde{t}^m), \nabla v) + (\nabla \Psi(\tilde{t}^{m-1}), \nabla v) \right) \\ &= -(\nabla \widehat{u}_H^m, \nabla v) - w_I^m - w_{II}^m + (\nabla u(\tilde{t}^{m-\frac{1}{2}}), \nabla v) + \mu(\nabla \Psi(\tilde{t}^{m-\frac{1}{2}}), \nabla v) \\ &\quad - \frac{\mu}{2} \left((\nabla \Psi(\tilde{t}^m), \nabla v) + (\nabla \Psi(\tilde{t}^{m-1}), \nabla v) \right) \\ &= (\nabla u(\tilde{t}^{m-\frac{1}{2}}) - \widehat{\nabla u}_H^m, \nabla v) - (w_I^m + w_{II}^m + \mu w_{III}^m, v), \end{aligned}$$

where w_I^m , w_{II}^m and w_{III}^m are defined by

$$w_I^m := (P_H^1 - I)\bar{\partial}\Psi(\tilde{t}^m), \quad w_{II}^m := \bar{\partial}\Psi(\tilde{t}^m) - \Psi_t(\tilde{t}^{m-\frac{1}{2}}), \quad \text{and } w_{III}^m := \Delta \psi(\tilde{t}^{m-\frac{1}{2}}) - \frac{1}{2}(\Delta \Psi(\tilde{t}^m) + \Delta \Psi(\tilde{t}^{m-1})). \quad (65)$$

Thus, (47) with a Crank-Nicolson scheme and with $v = \widehat{\theta}^m$ becomes

$$\begin{aligned} (\bar{\partial}\theta^m, \widehat{\theta}^m) + \mu(\nabla \widehat{\theta}^m, \nabla \widehat{\theta}^m) &= \frac{1}{\mu} (\bar{\partial}u_H^m - u_t(\tilde{t}^{m-\frac{1}{2}}), \widehat{\theta}^m) - (w_I^m + w_{II}^m + \mu w_{III}^m, \widehat{\theta}^m), \\ &= \frac{1}{\mu} (\bar{\partial}u_H^m - u_t(\tilde{t}^{m-\frac{1}{2}}), \widehat{\theta}^m) - (w_I^m, \widehat{\theta}^m), \end{aligned} \quad (66)$$

where $w_T^m = w_I^m + w_{II}^m + \mu w_{III}^m$. By definition of $\bar{\partial}$ (with the coarse time grid), and since the second term in (66) is always positive, we get

$$(\theta^m, \widehat{\theta^m}) - (\theta^{m-1}, \widehat{\theta^{m-1}}) \leq \Delta t_G \left[\frac{1}{\mu} \left\| \bar{\partial} u_H^m - u_t(\tilde{t}^{m-\frac{1}{2}}) \right\|_{L^2(\Omega)} + \|w_T^m\|_{L^2(\Omega)} \right] \left\| \widehat{\theta^m} \right\|_{L^2(\Omega)},$$

and by definition of $\widehat{\theta^m}$ (64),

$$\|\theta^m\|_{L^2(\Omega)}^2 - \|\theta^{m-1}\|_{L^2(\Omega)}^2 \leq \Delta t_G \left[\frac{1}{\mu} \left\| \bar{\partial} u_H^m - u_t(\tilde{t}^{m-\frac{1}{2}}) \right\|_{L^2(\Omega)} + \|w_T^m\|_{L^2(\Omega)} \right] \|\theta^m + \theta^{m-1}\|_{L^2(\Omega)},$$

so that, after cancellation of a common factor,

$$\|\theta^m\|_{L^2(\Omega)} - \|\theta^{m-1}\|_{L^2(\Omega)} \leq \Delta t_G \left[\frac{1}{\mu} \left\| \bar{\partial} u_H^m - u_t(\tilde{t}^{m-\frac{1}{2}}) \right\|_{L^2(\Omega)} + \|w_T^m\|_{L^2(\Omega)} \right],$$

and by recursive application, it entails

$$\|\theta^m\|_{L^2(\Omega)} \leq \underbrace{\frac{\Delta t_G}{\mu} \sum_{j=1}^m \left\| \bar{\partial} u_H^j - u_t(\tilde{t}^{j-\frac{1}{2}}) \right\|_{L^2(\Omega)}}_{T_{2,n}''} + \underbrace{\Delta t_G \sum_{j=1}^m \|w_T^j\|_{L^2(\Omega)}}_{T_{3,n}''}. \quad (67)$$

– To estimate $T_{2,n}''$, we use the same tricks as before (51). First, we can decompose $T_{2,n}''$ in 2 contributions, such that

$$\frac{\Delta t_G}{\mu} \sum_{j=1}^m \left\| \bar{\partial} u_H^j - u_t(\tilde{t}^{j-\frac{1}{2}}) \right\|_{L^2(\Omega)} \leq \frac{\Delta t_G}{\mu} \sum_{j=1}^m \underbrace{\left\| \bar{\partial} u_H^j - \bar{\partial} P_1^h u(\tilde{t}^j) \right\|_{L^2(\Omega)}}_{\|\bar{\partial} \theta_u^j\|_{L^2(\Omega)}} + \underbrace{\left\| \bar{\partial} P_1^h u(\tilde{t}^j) - u_t(\tilde{t}^{j-\frac{1}{2}}) \right\|_{L^2(\Omega)}}_{\|w_{I,u}^j + w_{II,u}^j\|_{L^2(\Omega)}},$$

where we denote by $w_{I,u}^m, w_{II,u}^m$ the same terms respectively defined by w_I^m, w_{II}^m (65) but with u instead of Ψ

$$w_{I,u}^m := (P_h^1 - I) \bar{\partial} u(\tilde{t}^m), \quad w_{II,u}^m := \bar{\partial} u(\tilde{t}^m) - u_t(\tilde{t}^{m-\frac{1}{2}}). \quad (68)$$

We now apply Cauchy-Schwarz inequality

$$\begin{aligned} \frac{\Delta t_G}{\mu} \sum_{j=1}^m \left\| \bar{\partial} u_H^j - u_t(\tilde{t}^{j-\frac{1}{2}}) \right\|_{L^2(\Omega)} &\leq \frac{\sqrt{\tilde{t}^m}}{\mu} \left[\left(\sum_{j=1}^m \Delta t_G \left\| \bar{\partial} \theta^j \right\|_{L^2(\Omega)}^2 \right)^{1/2} + \left(\sum_{j=1}^m \Delta t_G \left\| w_{I,u}^j + w_{II,u}^j \right\|_{L^2(\Omega)}^2 \right)^{1/2} \right], \\ &\leq \frac{\sqrt{\tilde{t}^m}}{\mu} \left[\left(\sum_{j=1}^m \Delta t_G \left\| \bar{\partial} \theta^j \right\|_{L^2(\Omega)}^2 \right)^{1/2} + \left(\sum_{j=1}^m \Delta t_G \left\| w_{I,u}^j + w_{II,u}^j \right\|_{L^2(\Omega)}^2 + \left\| w_{III,u}^j \right\|_{L^2(\Omega)}^2 \right)^{1/2} \right] \end{aligned} \quad (69)$$

* To estimate the first term of (69), we use $v = \bar{\partial} \theta_u^m$, and we now have (from the Crank-Nicolson scheme on u (11))

$$\left\| \bar{\partial} \theta_u^m \right\|_{L^2(\Omega)}^2 + \mu (\nabla \widehat{\theta_u^m}, \nabla \bar{\partial} \theta_u^m) = -(w_{I,u}^m + w_{II,u}^m + \mu w_{III,u}^m, \bar{\partial} \theta_u^m),$$

where

$$w_{III,u}^m := \Delta u(\tilde{t}^{m-\frac{1}{2}}) - \frac{1}{2} (\Delta u(\tilde{t}^m) + \Delta u(\tilde{t}^{m-1})), \quad (70)$$

and θ_u^m is the discrete version of (31). By definitions of $\bar{\partial}$ and $\widehat{\theta_u^m}$, it can be rewritten

$$\left\| \bar{\partial} \theta_u^m \right\|_{L^2(\Omega)}^2 + \frac{\mu}{2\Delta t_G} \left\| \nabla \theta_u^m \right\|_{L^2(\Omega)}^2 - \frac{\mu}{2\Delta t_F} \left\| \nabla \theta_u^{m-1} \right\|_{L^2(\Omega)}^2 = -(w_{I,u}^m + w_{II,u}^m + \mu w_{III,u}^m, \bar{\partial} \theta_u^m),$$

and it leads to (using Young's inequality)

$$\left\| \bar{\partial} \theta_u^m \right\|_{L^2(\Omega)}^2 + \frac{\mu}{\Delta t_G} \left\| \nabla \theta_u^m \right\|_{L^2(\Omega)}^2 - \frac{\mu}{\Delta t_G} \left\| \nabla \theta_u^{m-1} \right\|_{L^2(\Omega)}^2 \leq \left\| w_{I,u}^m + w_{II,u}^m + \mu w_{III,u}^m \right\|_{L^2(\Omega)}^2. \quad (71)$$

Now we find, as in (54) (by summing over all time steps in order to obtain a telescoping sum)

$$\sum_{j=1}^m \left\| \bar{\partial} \theta_u^j \right\|_{L^2(\Omega)}^2 \leq \frac{\mu}{\Delta t_G} \left\| \nabla \theta_u^j \right\|_{L^2(\Omega)}^2 + \sum_{j=1}^m \left\| w_{I,u}^j + w_{II,u}^j + w_{III,u}^j \right\|_{L^2(\Omega)}^2, \quad (72)$$

The term $\left\| \nabla \theta_u^m \right\|_{L^2(\Omega)}^2$ can easily be bounded by repeated application using (71). We find that (since the first term of (71) is positive)

$$\frac{\mu}{\Delta t_G} \left\| \nabla \theta_u^m \right\|_{L^2(\Omega)}^2 \leq \sum_{j=1}^m \left\| w_{I,u}^j + w_{II,u}^j + \mu w_{III,u}^j \right\|_{L^2(\Omega)}^2,$$

and thus (72) gives

$$\sum_{j=1}^m \left\| \bar{\partial} \theta_u^j \right\|_{L^2(\Omega)}^2 \leq 2 \sum_{j=1}^m \left\| w_{I,u}^j + w_{II,u}^j + \mu w_{III,u}^j \right\|_{L^2(\Omega)}^2 \leq 4 \sum_{j=1}^m \left\| w_{I,u}^j + w_{II,u}^j \right\|_{L^2(\Omega)}^2 + \left\| \mu w_{III,u}^j \right\|_{L^2(\Omega)}^2, \quad (73)$$

therefore we obtain for (69)

$$\frac{\Delta t_G}{\mu} \sum_{j=1}^m \left\| \bar{\partial} u_H^j - u_t(\tilde{t}^{j-\frac{1}{2}}) \right\|_{L^2(\Omega)} \leq 3\sqrt{\tilde{t}^m} \left[\left(\frac{\Delta t_G}{\mu^2} \sum_{j=1}^m \left\| w_{I,u}^j + w_{II,u}^j \right\|_{L^2(\Omega)}^2 + \sum_{j=1}^m \Delta t_G \left\| w_{III,u}^j \right\|_{L^2(\Omega)}^2 \right)^{1/2} \right],$$

which yields

$$\begin{aligned} \frac{\Delta t_G}{\mu} \sum_{j=1}^m \left\| \bar{\partial} u_H^j - u_t(\tilde{t}^{j-\frac{1}{2}}) \right\|_{L^2(\Omega)} &\leq 3\sqrt{\tilde{t}^m} \left[\left(\frac{2}{\mu^2} \sum_{j=1}^m \Delta t_G \left\| w_{I,u}^j \right\|_{L^2(\Omega)}^2 + \frac{2}{\mu^2} \sum_{j=1}^m \Delta t_G \left\| w_{II,u}^j \right\|_{L^2(\Omega)}^2 \right. \right. \\ &\quad \left. \left. + \sum_{j=1}^m \Delta t_G \left\| w_{III,u}^j \right\|_{L^2(\Omega)}^2 \right)^{1/2} \right]. \end{aligned} \quad (74)$$

* Now, we can estimate the right-hand side terms of (74) as done in [51]. We first remark that $w_{I,u}^j = w_{1,u}^j$ (and the estimate is given by (57) but with the coarse spatial and time grids), so it remains to seek bounds for $w_{II,u}^j$ and $w_{III,u}^j$.

• For $w_{II,u}^j$,

$$\begin{aligned} \Delta t_G \sum_{j=1}^m \left\| w_{II,u}^j \right\|_{L^2(\Omega)}^2 &= \frac{1}{\Delta t_G} \sum_{j=1}^m \left\| u(\tilde{t}^j) - u(\tilde{t}^{j-1}) - \Delta t_G u_t(\tilde{t}^{j-\frac{1}{2}}) \right\|_{L^2(\Omega)}^2, \\ &= \frac{1}{4\Delta t_G} \sum_{j=1}^m \left\| \int_{\tilde{t}^{j-1}}^{\tilde{t}^j} (s - \tilde{t}^{j-1})^2 u_{ttt}(s) + \int_{\tilde{t}^{j-\frac{1}{2}}}^{\tilde{t}^j} (s - \tilde{t}^j)^2 u_{ttt}(s) \, ds \right\|_{L^2(\Omega)}^2 \\ &\leq C\Delta t_G^3 \sum_{j=1}^m \left\| \int_{\tilde{t}^{j-1}}^{\tilde{t}^j} u_{ttt}(s) \, ds \right\|_{L^2(\Omega)}^2, \\ &\leq C\Delta t_G^4 \sum_{j=1}^m \int_{\tilde{t}^{j-1}}^{\tilde{t}^j} \|u_{ttt}\|_{L^2(\Omega)}^2 \, ds, \text{ with Cauchy-Schwarz inequality,} \\ &\leq C\Delta t_G^4 \int_0^{\tilde{t}^m} \|u_{ttt}\|_{L^2(\Omega)}^2 \, ds. \end{aligned} \quad (75)$$

• For $w_{III,u}^j$,

$$\begin{aligned}
\Delta t_G \sum_{j=1}^m \|w_{III,u}^j\|_{L^2(\Omega)}^2 &= \Delta t_G \sum_{j=1}^m \left\| \Delta u(\tilde{t}^{j-\frac{1}{2}}) - \frac{1}{2}(\Delta u(\tilde{t}^j) + \Delta u(\tilde{t}^{j-1})) \right\|_{L^2(\Omega)}^2, \\
&= \frac{\Delta t_G}{4} \sum_{j=1}^m \left\| \int_{\tilde{t}^{j-1}}^{\tilde{t}^{j-\frac{1}{2}}} (t^{j-1} - s) \Delta u_{tt}(s) \, ds + \int_{\tilde{t}^{j-\frac{1}{2}}}^{\tilde{t}^j} (s - \tilde{t}^j) \Delta u_{tt}(s) \, ds \right\|_{L^2(\Omega)}^2, \\
&\leq C \Delta t_G^3 \sum_{j=1}^m \left\| \int_{\tilde{t}^{j-1}}^{\tilde{t}^j} \Delta u_{tt} \, ds \right\|_{L^2(\Omega)}^2, \\
&\leq C \Delta t_G^4 \int_{\tilde{t}^0}^{\tilde{t}^m} \|\Delta u_{tt}\|_{L^2(\Omega)}^2 \, ds, \text{ by Cauchy-Schwarz inequality.} \tag{76}
\end{aligned}$$

Altogether,

$$T_{2,n}'' \leq C \left[\frac{H^2}{\mu} \left(\int_0^{\tilde{t}^m} \|u_t\|_{H^2(\Omega)}^2 \, ds \right)^{1/2} + \Delta t_G^2 \left(\left(\frac{1}{\mu} \int_0^{\tilde{t}^m} \|u_{ttt}\|_{L^2(\Omega)}^2 \, ds \right)^{1/2} + \left(\int_0^{\tilde{t}^m} \|\Delta u_{tt}\|_{L^2(\Omega)}^2 \, ds \right)^{1/2} \right] \right]. \tag{77}$$

– To estimate $T_{3,n}''$ defined in (67), we remark that $w_I^j = w_1^j$ (but with the coarse spatial and time grids), and

* for w_{II}^j ,

$$\begin{aligned}
\Delta t_G \|w_{II}^j\|_{L^2(\Omega)} &\leq \left\| \Psi(\tilde{t}^j) - \Psi(\tilde{t}^{j-1}) - \Delta t_G \Psi_t(\tilde{t}^{j-\frac{1}{2}}) \right\|_{L^2(\Omega)}, \\
&= \frac{1}{2} \left\| \int_{\tilde{t}^{j-1}}^{\tilde{t}^{j-\frac{1}{2}}} (s - \tilde{t}^{j-1})^2 \Psi_{ttt}(s) \, ds + \int_{\tilde{t}^{j-\frac{1}{2}}}^{\tilde{t}^j} (s - \tilde{t}^j)^2 \Psi_{ttt}(s) \, ds \right\|_{L^2(\Omega)} \\
&\leq C \Delta t_G^2 \int_{\tilde{t}^{j-1}}^{\tilde{t}^j} \|\Psi_{ttt}\|_{L^2(\Omega)} \, ds. \tag{78}
\end{aligned}$$

* Finally, for w_{III}^j ,

$$\Delta t_G \|w_{III}^j\|_{L^2(\Omega)} = \Delta t_G \left\| \Psi(\tilde{t}^{j-\frac{1}{2}}) - \frac{1}{2}(\Psi(\tilde{t}^j) + \Psi(\tilde{t}^{j-1})) \right\|_{L^2(\Omega)} \leq C \Delta t_G^2 \int_{\tilde{t}^{j-1}}^{\tilde{t}^j} \|\Delta \Psi_{tt}\|_{L^2(\Omega)} \, ds. \tag{79}$$

Altogether,

$$T_{3,n}'' \leq CH^2 \int_0^{\tilde{t}^m} \|\Psi_t\|_{H^2(\Omega)} \, ds + C \Delta t_G^2 \int_0^{\tilde{t}^m} \left(\|\Psi_{ttt}\|_{L^2(\Omega)} + \mu \|\Delta \Psi_{tt}\|_{L^2(\Omega)} \right) \, ds, \tag{80}$$

which concludes the proof (combining (67), (77) and (80)). \square

In analogy with the previous work on parabolic equations, we define

$$\widetilde{\Psi}_H^n = I_n^2[\Psi_H^m](\mu), \quad \text{for } n = 0, \dots, N_T, \tag{81}$$

with I_n^2 defined by (12) as the quadratic interpolation in time of the coarse solution at time $t^n \in I_m = [\tilde{t}^{m-1}, \tilde{t}^m]$ defined on $[\tilde{t}^{m-2}, \tilde{t}^m]$ from the values $\Psi_H^{m-2}, \Psi_H^{m-1}$, and Ψ_H^m , for all $m = 2, \dots, M_T$. For $t^n \in I_1 = [\tilde{t}^0, \tilde{t}^1]$, we use the same parabola defined by the values $\Psi_H^0, \Psi_H^1, \psi_H^2$ as the one used over $[\tilde{t}^1, \tilde{t}^2]$. Note that, as before, we could have chosen another quadratic interpolation.

Corollary 2.11 (of Theorem 2.10). *Under the assumptions of Theorem 2.10, let u_H^m be the fully-discretized solution (11) on the coarse mesh \mathcal{T}_H . Let Ψ and Ψ_H^m be the corresponding sensitivities, respectively given by (23) and by (63). Let $\widetilde{\Psi}_H^n$ be the quadratic interpolation of the coarse solution Ψ_H^m given by (81). Then,*

$$\begin{aligned}
\forall n = 0, \dots, N_T, \quad \left\| \widetilde{\Psi}_H^n - \Psi(t^n) \right\|_{L^2(\Omega)} &\leq CH^2 \left[\left\| \Psi^0 \right\|_{H^2(\Omega)} + \int_0^{t^n} \|\Psi_t\|_{H^2(\Omega)} \, ds + C(\mu) \left[\int_0^{t^n} \|u_t\|_{H^2(\Omega)}^2 \, ds \right]^{1/2} \right] \\
&\quad + C \Delta t_G^2 \left(\int_0^{t^n} \|\Psi_{ttt}\|_{L^2(\Omega)} \, ds + \left[\int_0^{t^n} \|\Delta u_{tt}\|_{L^2(\Omega)}^2 \, ds \right]^{1/2} + C(\mu) \left[\int_0^{t^n} \|u_{ttt}\|_{L^2(\Omega)}^2 \, ds \right]^{1/2} + \int_0^{t^n} \|\Delta \Psi_{tt}\|_{L^2(\Omega)} \, ds \right).
\end{aligned}$$

In the next section, we proceed with the adjoint state formulation.

2.4 Sensitivity analysis: The adjoint problem.

The adjoint method may be seen as an inverse method, where we aim at retrieving the optimal parameter of an objective function \mathcal{F} . The latter will have a different meaning whether the goal is to retrieve the parameters from several measures (for parameter identification) or if we want to optimize a function depending on the variables (PDE-constrained optimization). In the first case, \mathcal{F} will have the following form (in its fully-discretized version)

$$\mathcal{F}(\mu) = \frac{1}{2} \sum_{n=0}^{N_T} \underbrace{\|u_h^n(\mu) - \bar{u}^n\|_{L^2(\Omega)}^2}_{\|err(t^n; \mu)\|_{L^2(\Omega)}^2}, \quad (82)$$

where the term \bar{u}^n refers to the measures which may be noisy (here for simplicity we consider the case of measures on the variables although it may be given by other outputs). In the second case, it will be written

$$\mathcal{F}(\mu) = \sum_{n=0}^{N_T} g^n u_h^n(\mu),$$

with g^n are some suitable weights. Note that by differentiating \mathcal{F} with respect to the parameters μ_p , $p = 1, \dots, P$, we can observe the influence on the objective function of the input parameters through the normalized sensitivity coefficients (also called elasticity of \mathcal{P}) [4]

$$S_k = \frac{\partial \mathcal{F}}{\partial \mu_k}(\mu) \times \frac{\mu_k}{\mathcal{F}(\mu)}, \quad k = 1, \dots, P.$$

2.4.1 The continuous setting.

- Let us for instance consider the first case outlined above given in its continuous version by

$$\mathcal{F}(\mu) = \frac{1}{2} \int_0^T \|err(t; \mu)\|_{L^2(\Omega)}^2 dt. \quad (83)$$

- To minimize \mathcal{F} under the constraint that " u is the solution of our model problem (3)", we consider the following Lagrangian with (χ, φ) the Lagrangian multipliers

$$\mathcal{L}(u, \chi, \varphi; \mu) = \mathcal{F}(\mu) + \int_0^T (\chi, (\nabla \cdot (A(\mu) \nabla u) + f - u_t)) ds + \int_0^T (\varphi, u)_{L^2(\partial\Omega)} ds, \quad (84)$$

where

- $\chi \in V$ is the multiplier associated to the constraint " u is a solution of (3)",
- $\varphi \in \mathbb{R}$ is the multiplier associated to the constraint of the Dirichlet boundary condition on $\partial\Omega$. Since here we consider homogeneous condition, we just impose $\varphi = 0$.
- Differentiating \mathcal{L} with respect to the parameter μ_p , for $p = 1, \dots, P$, we obtain the following adjoint system in its variational form (see A for more details)

$$\begin{cases} \text{Find } \chi(t) \in V \text{ for } t \in [0, T] \text{ such that} \\ (\chi_t(t), v) = -(\frac{\partial err}{\partial u}(t; \mu), v) + (A(\mu) \nabla \chi(t), \nabla v), \quad \forall v \in V, t < T, \\ \chi(\cdot, T) = 0, \text{ in } \Omega. \end{cases} \quad (85)$$

- After solving (85) with the parameter μ , one can compute the sensitivities of the objective function $\frac{d\mathcal{F}}{d\mu_p}$ by noticing that

$$\frac{d\mathcal{F}}{d\mu_p} = \frac{d\mathcal{L}}{d\mu_p} = \int_0^T \left(\chi, \nabla \cdot \left(\frac{\partial A}{\partial \mu_p}(\mu) \nabla u \right) \right) ds, \text{ from (129)}. \quad (86)$$

Remark 2.12. For a stable implementation, one may have to add a regularization term depending of the parameter to the cost function $\mathcal{F}(p)$.

2.4.2 Discretized setting.

In analogy with the direct method, we first discretize the system (85) in space, and then apply an Euler scheme with the fine grids and the Crank-Nicolson method with the coarse ones. The semi-discretized version on \mathcal{T}_h writes

$$\left\{ \begin{array}{l} \text{Find } \chi_h(t) \in V_h \text{ for } t \in [0, T] \text{ such that} \\ (\chi_{h,t}(t), v_h) - a(\chi_h, v_h; \mu) = -(\frac{\partial \text{err}_h}{\partial u_h}(t; \mu), v_h), \forall v_h \in V_h, t < T, \\ \chi_h(\cdot, T) = 0, \text{ in } \Omega. \end{array} \right. \quad (87)$$

With the fully-discretized version on the fine grids, the adjoint system (87) becomes

$$\left\{ \begin{array}{l} \text{Find } \chi_h^n \in V_h \text{ for } n \in \{0, \dots, N_T\} \text{ such that} \\ (\bar{\partial} \chi_h^n, v_h) - a(\chi_h^n, v_h; \mu) = -(u_h^n - \bar{u}^n, v_h), \forall n = 0, \dots, N_T - 1, \\ \chi_h^{N_T}(\cdot) = 0. \end{array} \right. \quad (88)$$

Note that to compute $\frac{\partial \text{err}_h^n}{\partial u_h}$, we need the fine solutions u_h^n and the associated measures. As for the state variable (11), we also compute the adjoint on the coarse mesh with the Crank-Nicolson scheme,

$$\left\{ \begin{array}{l} \text{Find } \chi_H^m \in V_H \text{ for } m \in \{0, \dots, M_T\} \text{ such that} \\ (\bar{\partial} \chi_H^m, v_H) - a(\widehat{\chi}_H^m, v_H; \mu) = -\frac{1}{2} \left((u_H^m - \bar{u}^m, v_H) + (u_H^{m-1} - \bar{u}^{m-1}, v_H) \right), \forall m = 0, \dots, M_T - 1, \\ \chi_H^{M_T}(\cdot) = 0, \end{array} \right. \quad (89)$$

with

$$\widehat{\chi}_H^m = \frac{1}{2}(\chi_H^m + \chi_H^{m-1}).$$

Finally, note that the problems (88) and (89) are well-posed, since they are solved backward in time (see [17] for precisions in the general setting of time-dependent PDEs).

3 NIRB algorithms applied to sensitivity analysis

In this section, we propose several adaptations of the NIRB two-grid algorithm to the context of sensitivity analysis with the direct and adjoint formulations.

3.1 On the direct problem.

3.1.1 Adapted NIRB algorithm.

Let $u(\mu)$ be the exact solution of problem (3) for a parameter $\mu \in \mathcal{G}$ and $\Psi_p(\mu)$ its sensitivity with respect to the parameter μ_p , $p = 1, \dots, P$. We consider P parameters of interest. In this context, we use the following offline/online decomposition for the NIRB procedure:

- “Offline part”

1. For a set of training parameters $(\tilde{\mu}_i)_{i=1, \dots, N_{p, \text{train}}}$, we define $\mathcal{G}_{p, \text{train}} = \bigcup_{i \in \{1, \dots, N_{p, \text{train}}\}} \tilde{\mu}_i$. Then, through a greedy algorithm 1, we adequately choose the parameters of the RB. During this procedure, we compute fine fully-discretized solutions $\{\Psi_{p,h}^n(\tilde{\mu}_i)\}_{i \in \{1, \dots, N_{\mu,p}\}, n \in \{0, \dots, N_T\}}$ ($N_{\mu,p} \leq N_{p, \text{train}}$) with the HF solver, by solving either (44) or the following problem (where u_h^n in (44) has been replaced by its NIRB approximation $u_{Hh}^{N,n}$ or by its rectified version $\mathbf{R}_u^n[u_{Hh}^{N,n}]$ obtained from the algorithm of section 2.2)

$$\left\{ \begin{array}{l} \text{Find } \Psi_{p,h}^n \in V_h \text{ for } n \in \{0, \dots, N_T\} \text{ such that} \\ (\bar{\partial} \Psi_{p,h}^n, v_h) + a(\Psi_{p,h}^n, v_h; \tilde{\mu}) = -(\frac{\partial A}{\partial \mu_p}(\mu) \nabla u_{Hh}^{N,n}(\mu), \nabla v_h) \text{ for } n = \{1, \dots, N_T\}, \\ \Psi_{p,h}^0(\cdot; \tilde{\mu}) = P_h^1 \Psi_p^0(\cdot; \tilde{\mu}). \end{array} \right. \quad (90)$$

The term $-(\frac{\partial A}{\partial \mu_p}(\mu) \nabla u_{Hh}^{N,n}(\mu), \nabla v_h)$ in (90) is replaced by $-(\frac{\partial A}{\partial \mu_p}(\mu) \nabla \mathbf{R}_u^n[u_{Hh}^{N,n}](\mu), \nabla v_h)$ in case of the rectification post-treatment (19). Note that u_h^n can directly be used (as in (44)) since this step belongs to the offline part of the NIRB algorithm. However, if the number of parameters required for the initial RB is lower than the number of parameters needed for the sensitivities RB or if one combine the sensitivities with an optimization algorithm, it may be convenient to employ (90) instead of (44). In analogy with section 2.2, a few time steps may be selected for each parameter of the RB, and thus, we obtain N_p L^2 orthogonal RB (time-independent) functions, denoted $(\zeta_{p,i}^h)_{i=1,\dots,N_p}$, and the reduced spaces $X_{p,h}^{N_p} := \text{Span}\{\zeta_{p,1}^h, \dots, \zeta_{p,N_p}^h\}$ for $p = 1, \dots, P$.

2. Then, for each p , we solve the eigenvalue problem (14) on $X_{p,h}^{N_p}$:

$$\begin{cases} \text{Find } \zeta^h \in X_{p,h}^{N_p}, \text{ and } \lambda \in \mathbb{R} \text{ such that:} \\ \forall v \in X_{p,h}^{N_p}, \int_{\Omega} \nabla \zeta^h \cdot \nabla v \, d\mathbf{x} = \lambda \int_{\Omega} \zeta^h \cdot v \, d\mathbf{x}. \end{cases} \quad (91)$$

For each parameter $p \in \{1, \dots, P\}$, we get an increasing sequence of eigenvalues λ_i^p , and eigenfunctions $(\zeta_{p,i}^h)_{i=1,\dots,N_p}$, orthonormalized in $L^2(\Omega)$ and orthogonalized in $H^1(\Omega)$.

3. As in the offline step 3 from section 2.2, we enhance the NIRB approximation with a rectification post-processing. Thus, we introduce the rectification matrices, denoted $\mathbf{R}_{\Psi}^{p,n}$. They are associated to the sensitivities problem (44), defined for each $p \in \{1, \dots, P\}$ and each fine time step $n \in \{0, \dots, N_T\}$, and constructed from coarse snapshots, generated by solving (63) and whose parameters are the same as for the fine snapshots.

Thus, for all $n = 0, \dots, N_T$ and all $p = 1, \dots, P$, we compute the vectors

$$\mathbf{R}_{\Psi,i}^{p,n} = ((\mathbf{A}^{p,n})^T \mathbf{A}^{p,n} + \delta_p \mathbf{I}_{N_p})^{-1} (\mathbf{A}^{p,n})^T \mathbf{B}_i^{p,n}, \quad i = 1, \dots, N_p, \quad (92)$$

where

$$\forall i = 1, \dots, N_p, \quad \text{and} \quad \forall \tilde{\mu}_k \in \mathcal{G}_p, \quad (93)$$

$$A_{k,i}^{p,n} = \int_{\Omega} \widetilde{\Psi_{p,H}^n}(\tilde{\mu}_k) \cdot \zeta_{p,i}^h \, d\mathbf{x},$$

$$B_{k,i}^{p,n} = \int_{\Omega} \Psi_{p,h}^n(\tilde{\mu}_k) \cdot \zeta_{p,i}^h \, d\mathbf{x}, \quad (94)$$

and where \mathbf{I}_{N_p} refers to the identity matrix and δ_p is a regularization term (note that we used (81) for $\widetilde{\Psi_{p,H}^n}(\tilde{\mu}_k)$).

Remark 3.1. In general, $N_{p,\text{train}} < N_p$ and the parameter δ_p is required for the inversion of $(\mathbf{A}^{p,n})^T \mathbf{A}^{p,n}$.

- “Online part”

The online part of the algorithm is much faster than a double HF evaluation (to seek the sensitivity $\Psi_{p,h}^n$, we also need the solution u_h^n with a HF evaluation).

4. Indeed, we first solve the problem (3) on the coarse mesh \mathcal{T}_H for a new parameter $\mu \in \mathcal{G}$ at each time step $m = 0, \dots, M_T$ using (11).
5. Then, for each $p = 1, \dots, P$, we solve the coarse associated sensitivity problems (63) with the same parameter μ , at each time step $m = 0, \dots, M_T$.
6. We quadratically interpolate in time the coarse solution $\Psi_{p,H}^m$ on the fine time grid with (81).
7. Then, we linearly interpolate $\widetilde{\Psi_{p,H}^n}(\mu)$ on the fine mesh in order to compute the L^2 -inner product with the basis functions. The approximation used in the two-grid method is

$$\text{For } n = 0, \dots, N_T, \quad \Psi_{p,Hh}^{N_p,n}(\mu) := \sum_{i=1}^{N_p} (\widetilde{\Psi_{p,H}^n}(\mu), \zeta_{p,i}^h) \zeta_{p,i}^h, \quad (95)$$

and with the rectification post-treatment step, it becomes

$$\mathbf{R}_{\Psi}^{p,n}[\Psi_{p,Hh}^N](\mu) := \sum_{i,j=1}^{N_p} R_{ij}^{p,n}(\widetilde{\Psi}_{p,H}^n(\mu), \zeta_{p,j}^h) \zeta_{p,i}^h, \quad (96)$$

where $\mathbf{R}_{\Psi}^{p,n}$ is the rectification matrix at time t^n , given by (92).

In the next section, we propose a NIRB two-grid algorithm with a new post-treatment which reduces the online computational time.

3.1.2 GP NIRB two-grid algorithm for the direct problem.

The main drawback of the algorithm described in the previous section is that it requires $1 + P$ coarse systems in the online part (see the steps 4 and 5 in section 3.1.1). The online portion of the new algorithm described below only requires the resolution of one coarse problem, regardless of the number of parameters of interest. The idea is to construct a learning post-treatment between the coarse and the fine coefficients as in [19] with different RB but here through a Gaussian Process Regression (GPR) [21, 44] instead of a deterministic procedure. We adapt the Gaussian Processes (GP) employed in [22] by using the coarse coefficients as inputs of our GP instead of the time steps and parameters. As a result, we have chosen another kernel for the covariance function and we consider time-independent RB functions. This new non-intrusive algorithm is simple to implement and it may yield very good performance in both accuracy and efficiency for time-dependent problems applied to sensitivity analysis, as shown in section 5.

We refer to the following offline/online decomposition:

- “Offline part”

1. From a parameter training set \mathcal{G}_{train} , we seek the RB parameters $(\mu_1, \dots, \mu_N) \in \mathcal{G}_N$ for the problem solutions through the greedy algorithm 1.
2. Meanwhile, we similarly find the RB parameters in \mathcal{G}_p for the sensitivities from the training sets $\mathcal{G}_{p,train}$ for $p = 1, \dots, P$. We denote by $\mathcal{G}_{T,train} := \mathcal{G}_{train} \cup \mathcal{G}_{p,train}$ the set of all training parameters, and denote by $N_{T,train}$ its cardinality. Then, in order to represent well all the solution manifolds with the same parameters, we define \mathcal{G}_T by

$$\mathcal{G}_T := \mathcal{G}_N \cup \mathcal{G}_p, \quad (97)$$

and $N_{\mu,T}$ the number of parameters in \mathcal{G}_T . Then, we generate the reduced spaces $X_h^{N_{\mu,T}}$ and $X_{p,h}^{N_{\mu,T}}$ (resp. of the solutions and of the sensitivities) using steps 1 and 2 of section 3.1.1. At the end of this part, we obtain $N_{\mu,T}$ RB functions for the problem solutions denoted $(\Phi_i^n)_{i=1, \dots, N_{\mu,T}}$ and $N_{\mu,T}$ RB functions for the sensitivities, denoted $(\zeta_{p,i}^h)_{i=1, \dots, N_{\mu,T}}$ for each $p = 1, \dots, P$.

3. **Gaussian Process Regression (GPR).**

We then use the fact that the sensitivities are directly derived from the initial solutions, and thus, we consider a Gaussian metamodel to recover the fine coefficients of the sensitivities (99) from the coarse coefficients of the problem solutions (98). In addition to the fine sensitivity coefficients already computed for the RB generation, we compute the coarse coefficients for the problem solutions. Thus, we define

$$\forall \tilde{\mu}_k \in \mathcal{G}_T, \forall i = 1, \dots, N_{\mu,T}, \forall n = 0, \dots, N_T, \quad A_i^n(\tilde{\mu}_k) = \int_{\Omega} \widetilde{u}_H^n(\tilde{\mu}_k) \cdot \Phi_i^h \, d\mathbf{x}, \quad (98)$$

$$B_i^{p,n}(\tilde{\mu}_k) = \int_{\Omega} \Psi_{p,h}^n(\tilde{\mu}_k) \cdot \zeta_{p,i}^h \, d\mathbf{x}, \quad (99)$$

and use them as a set of inputs-outputs for our GPR model,

$$\mathcal{D} = \{(\mathbf{A}_k, \mathbf{B}_k) : k = 1, \dots, N_{T,train}\}, \quad (100)$$

with $\mathbf{A}_k = (A_i^n(\tilde{\mu}_k))_{n=0,\dots,N_T, i=1,\dots,N_{\mu,T}}$ and $\mathbf{B}_k = (B_i^n(\tilde{\mu}_k))_{n=0,\dots,N_T, i=1,\dots,N_{\mu,T}}$ for $k = 1, \dots, N_{T,train}$. We denote by $\mathbf{A} = \{\mathbf{A}_1, \dots, \mathbf{A}_{N_{T,train}}\}$ the training inputs and by $\mathbf{B} = \{\mathbf{B}_1, \dots, \mathbf{B}_{N_{T,train}}\}$ the associated outputs.

Here, we deal with 3 kinds of indices:

- the number of modes: $N_{\mu,T}$,
- the cardinality of the parameters training set: $N_{T,train}$,
- and the number of time steps which is $N_T + 1$.

The observed input-output pairs in \mathcal{D} are assumed to follow some unknown regression function

$$f : \mathbb{R}^{N_{\mu,T} \times (N_T+1)} \rightarrow \mathbb{R}^{N_{\mu,T} \times (N_T+1)}, f(\mathbf{A}_k) = \mathbf{B}_k, k = 1, \dots, N_{T,train}.$$

From a Bayesian perspective, we can define a prior and posterior GP on the regression:

- the prior GP reflects our beliefs about the metamodel before seeing any training data, and is solely defined by a mean and a covariance function;
- the posterior GP conditioned the prior on the training data, i.e. includes the knowledge from the data \mathcal{D} .

Let the prior GP be corrupted by an independent Gaussian noise term, i.e.

$$\text{for } (\mathbf{x}, \mathbf{x}') \in \mathbb{R}^{N_{\mu,T} \times (N_T+1)} \times \mathbb{R}^{N_{\mu,T} \times (N_T+1)}, f(\mathbf{x}) \sim GP(0, \kappa(\mathbf{x}, \mathbf{x}')), \mathbf{y} = f(\mathbf{x}) + \epsilon, \text{ where } \epsilon \sim \mathcal{N}(0, \sigma_y^2),$$

where the covariance function κ is a positive definite kernel (see [14] for an overview on different kernels). There are many different options for the covariance functions. In our setting we use the standard squared exponential covariance function (also known as radial basis function)

$$\text{for } (\mathbf{x}, \mathbf{x}') \in \mathbb{R}^{N_{\mu,T} \times (N_T+1)} \times \mathbb{R}^{N_{\mu,T} \times (N_T+1)}, \kappa(\mathbf{x}, \mathbf{x}') = \sigma_f^2 \exp\left(-\frac{1}{2l^2} \|\mathbf{x} - \mathbf{x}'\|^2\right), \quad (101)$$

with $\|\cdot\|$ being the usual Euclidean norm and where two hyperparameters are employed: the standard deviation parameter σ_f and the correlated length-scale l . We assume that the prior mean function is zero which is common practice and does not limit the GP model.

The goal of GPR is then to use the training data \mathcal{D} (100) to make predictions when given new inputs. In our case, those new points (where we predict the output) will be the coarse coefficients given by (98) for a new parameter $\mu \in \mathcal{G}$.

To incorporate our knowledge from the training data, we condition the prior GP on our set of training data points \mathcal{D} (100). The posterior distribution of the output f^* for a new input $\mathbf{A}^* \in \mathbb{R}^{N_{\mu,T} \times (N_T+1)}$ is then given by [54]

$$\begin{aligned} f^* | \mathbf{A}^*, \mathbf{A}, \mathbf{B} &\sim \mathcal{N}(m^*(\mathbf{A}^*), C^*(\mathbf{A}^*, \mathbf{A}^*)), \\ \text{with } m^*(\mathbf{A}^*) &= K^{*T} K_y^{-1} \mathbf{B}, \\ \text{and } C^*(\mathbf{A}^*, \mathbf{A}^*) &= K^{**} - K^{*T} K_y^{-1} K^*, \end{aligned} \quad (102)$$

where $K_y = \kappa(\mathbf{A}, \mathbf{A}) + \sigma_y^2 \mathbf{I}_{N_{T,train}}$ ($\mathbf{I}_{N_{T,train}}$ being the $N_{T,train}$ -dimensional unit matrix), $K^* = \kappa(\mathbf{A}^*, \mathbf{A})$ and $K^{**} = \kappa(\mathbf{A}^*, \mathbf{A}^*)$.

The hyperparameters $\theta = (\sigma_f, l)$ in (101) are optimised by maximising the log marginal likelihood using a gradient-based optimiser. The log marginal likelihood is given by

$$\theta_{opt} \in \arg \max_{\theta} \log p(\mathbf{B} | \mathbf{A}) = \arg \max_{\theta} \left\{ -\frac{1}{2} \mathbf{B}^T K_y^{-1}(\theta) \mathbf{B} - \frac{1}{2} \log |K_y(\theta)| - \frac{N_{T,train}}{2} \log(2\pi) \right\},$$

where $p(\mathbf{B} | \mathbf{A})$ is the conditional density function of \mathbf{B} given \mathbf{A} , also considered as the log marginal likelihood. Note that computing the inverse of K_y may be computationally expensive, i.e. on the order $\mathcal{O}(N_{T,train}^3)$, increasing the offline computational cost when the number of training samples increases. Yet, we get rid of the time complexity since we employ a "global" GP on time and the covariance function defined by (101).

- “Online step”

4. We solve the problem (3) on the coarse mesh \mathcal{T}_H for a new parameter $\mu \in \mathcal{G}$ at each time step $m = 0, \dots, M_T$ using (11).
5. We quadratically interpolate in time the coarse solution u_H^m on the fine time grid with (12).
6. Then, we linearly interpolate $\widetilde{u}_H^n(\mu)$ on the fine mesh in order to compute the L^2 -inner product with the basis functions. We derive the new coarse coefficients with

$$A_j^n(\mu) = (\widetilde{u}_H^n(\mu), \Phi_j^h) \text{ for } j = 1, \dots, N_{\mu,T} \text{ and } n = 0, \dots, N_T. \quad (103)$$

We denote by $\mathbf{A}^*(\mu)$ these coefficients. Then, the new sensitivity fine coefficients \mathbf{B}^{GP} are approximated following (102), thus

$$\mathbf{B}^{GP}(\mathbf{A}^*(\mu)) \sim GP(m^*(\mathbf{A}^*(\mu)), C^*(\mathbf{A}^*(\mu), \mathbf{A}^*(\mu))),$$

with m^* and C^* defined by (102). Finally, the new NIRB approximation is obtained by

$$\Psi_{p,Hh}^{GP,n}(\mu) := \sum_{i=1}^{N_{\mu,T}} [\mathbf{B}^{GP}(\mathbf{A}^*(\mu))]_i^n \zeta_{p,i}^h. \quad (104)$$

Now, we proceed with the NIRB two-grid algorithm adapted to the adjoint formulation.

3.2 On the adjoint formulation.

The adjoint formulation requires some modifications of the NIRB two-grid algorithm presented in section 3.1.1. Since in (86), for all $n \in \{0, \dots, N_T\}$, the fine solution $u_h^n(\mu)$ is required to obtain the sensitivities on \mathcal{F} , it follows that here we have to compute two reductions: one for the initial solution u and one for the adjoint χ . As a matter of fact, in (3.1.1), the RB generation for u was optional.

So let $u(\mu)$ be the exact solution of problem (3) for a parameter $\mu \in \mathcal{G}$ and $\chi(\mu)$ its adjoint given by (85). In this setting, we use the following offline/online decomposition for the NIRB procedure:

- “Offline part”

1. During the offline stage, we first construct the reduced space X_h^N and the RB function $(\Phi_1^h, \dots, \Phi_N^h)$ with the steps 1-2 of section 2.2.
2. Then, we use steps 1-2 of section 3.1.1, but instead of solving (44) on the sensitivities, we generate the reduced space $X_1^{N_1}$ by solving the adjoint problem on the fine mesh (88).

Thus, for a set of training parameters $(\tilde{\mu}_i)_{i=1, \dots, N_{1,train}}$, we define $\mathcal{G}_{1,train} = \bigcup_{i \in \{1, \dots, N_{1,train}\}} \tilde{\mu}_i$. Then,

through a greedy procedure 1, we adequately choose the parameters of the RB. During this procedure, we compute fine fully-discretized solutions $\{\chi_h^n(\tilde{\mu}_i)\}_{i \in \{1, \dots, N_{\mu,1}\}, n \in \{0, \dots, N_T\}}$ ($N_{\mu,1} \leq N_{1,train}$) with the HF solver, by solving either (88) or the following problem (where u_h^n in (88) has been replaced by its NIRB approximation $u_{Hh}^{N,n}$ or by its rectified version $\mathbf{R}_u^N[u_{Hh}^{N,n}]$ obtained from the algorithm of section 2.2)

$$\begin{cases} \text{Find } \chi_h^n \in V_h \text{ for } n \in \{0, \dots, N_T\} \text{ such that} \\ (\bar{\partial} \chi_h^n, v_h) - a(\chi_h, v_h; \mu) = -(u_{Hh}^{N,n} - \bar{u}^n, v_h), \quad \forall n = 0, \dots, N_T - 1, \\ \chi_h^{N_T}(\cdot) = 0. \end{cases} \quad (105)$$

The term $-(u_{Hh}^{N,n}(\mu) - \bar{u}^n, v_h)$ in (105) is replaced by $-(\mathbf{R}_u^N[u_{Hh}^{N,n}](\mu) - \bar{u}^n, v_h)$ in case of the rectification post-treatment (19). In practice, since in step 1 a RB for u_h^n has already been generated, it is more convenient to employ (105) instead of (88).

In analogy with section 2.2, a few time steps may be selected for each parameter of the RB, and thus, we obtain N_1 L^2 orthogonal RB (time-independent) functions, denoted $(\zeta_i^h)_{i=1, \dots, N_1}$, and the reduced space $X_h^{N_1} := \text{Span}\{\zeta_1^h, \dots, \zeta_{N_1}^h\}$.

3. Then, we solve the eigenvalue problem (14) on $X_h^{N_1}$:

$$\begin{cases} \text{Find } \zeta^h \in X_h^{N_1}, \text{ and } \lambda \in \mathbb{R} \text{ such that:} \\ \forall v \in X_h^{N_1}, \int_{\Omega} \nabla \zeta^h \cdot \nabla v \, d\mathbf{x} = \lambda \int_{\Omega} \zeta^h \cdot v \, d\mathbf{x}. \end{cases} \quad (106)$$

We get an increasing sequence of eigenvalues λ_i , and eigenfunctions $(\zeta_i^h)_{i=1, \dots, N_1}$, orthonormalized in $L^2(\Omega)$ and orthogonalized in $H^1(\Omega)$.

4. As in the offline step 3 from section 3.1.1, we enhance the NIRB approximation with a rectification post-processing. Thus, we introduce a rectification matrix, denoted \mathbf{R}_{χ}^n for each fine time step $n \in \{0, \dots, N_T\}$. It is associated to the adjoint problem (88) and constructed from coarse snapshots, generated by solving (89) and whose parameters are the same as for the fine snapshots. Thus, for all $n = 0, \dots, N_T$, we compute the vectors

$$\mathbf{R}_{\chi,i}^n = ((\mathbf{A}^n)^T \mathbf{A}^n + \delta \mathbf{I}_{N_1})^{-1} (\mathbf{A}^n)^T \mathbf{B}_i^n, \quad i = 1, \dots, N_1, \quad (107)$$

where

$$\forall i = 1, \dots, N_1, \quad \text{and} \quad \forall \tilde{\mu}_k \in \mathcal{G}_p,$$

$$A_{k,i}^n = \int_{\Omega} \tilde{\chi}_H^n(\tilde{\mu}_k) \cdot \zeta_i^h \, d\mathbf{x}, \quad (108)$$

$$B_{k,i}^n = \int_{\Omega} \chi_h^n(\tilde{\mu}_k) \cdot \zeta_i^h \, d\mathbf{x}, \quad (109)$$

and where \mathbf{I}_{N_1} refers to the identity matrix and δ_p is a regularization term required for the inversion of $(\mathbf{A}^n)^T \mathbf{A}^n$ (note that we used (81) for $\tilde{\chi}_H^n(\tilde{\mu}_k)$).

• “Online part”

4. We first solve the problem (3) on the coarse mesh \mathcal{T}_H for a new parameter $\mu \in \mathcal{G}$ at each time step $m = 0, \dots, M_T$ using (11).
5. Then, we solve the coarse associated adjoint problem (89) with the same parameter μ , at each time step $m = 0, \dots, M_T$.
6. We quadratically interpolate in time the coarse solution χ_H^m on the fine time grid with (81).
7. Then, we linearly interpolate $\tilde{\chi}_H^n(\mu)$ on the fine mesh in order to compute the L^2 -inner product with the basis functions. The approximation used for the adjoint in the two-grid method is

$$\text{For } n = 0, \dots, N_T, \quad \chi_{Hh}^{N_1,n}(\mu) := \sum_{i=1}^{N_1} (\tilde{\chi}_H^n(\mu), \zeta_i^h) \zeta_i^h, \quad (110)$$

and with the rectification post-treatment step, it becomes

$$\mathbf{R}_{\chi}^n[\chi_{Hh}^{N_1}](\mu) := \sum_{i,j=1}^{N_1} R_{\chi,ij}^n (\tilde{\chi}_H^n(\mu), \zeta_j^h) \zeta_i^h, \quad (111)$$

where \mathbf{R}_{χ}^n is the rectification matrix at time t^n , given by (107).

8. Then, we use the steps 5 and 6 of section 2.2 in order to obtain a NIRB approximation for $u(\mu)$ from the coarse solution u_H^m given by step 4 of this online part.
9. Finally, the sensitivities NIRB approximations of \mathcal{F} are given by

$$\text{for } p = 1, \dots, P, \quad \left[\frac{\partial \mathcal{F}}{\partial \mu_p} \right]_{Hh}^{N_1}(\mu) := \sum_{j=1}^{t^n} \Delta t_F \left(\chi_{Hh}^{N_1,j}, \nabla \cdot \left(\frac{\partial A}{\partial \mu_p}(\mu) \nabla u_{Hh}^{N,j} \right) \right), \text{ from (86),} \quad (112)$$

and with the rectification post-treatment step, it becomes

$$\text{for } p = 1, \dots, P, \quad \mathbf{R}_{\chi} \left[\left[\frac{\partial \mathcal{F}}{\partial \mu_p} \right]_{Hh}^{N_1} \right](\mu) := \sum_{j=1}^{t^n} \Delta t_F \left(\mathbf{R}_{\chi}^j[\chi_{Hh}^{N_1,j}](\mu), \nabla \cdot \left(\frac{\partial A}{\partial \mu_p}(\mu) \nabla \mathbf{R}_u^j[u_{Hh}^{N,j}](\mu) \right) \right). \quad (113)$$

The next section gives our main result on the NIRB two-grid method error estimate in the context of sensitivity analysis.

4 NIRB error estimate on the sensitivities

Main result Our main theoretical result is the following theorem, which applies to the direct sensitivity formulation.

Theorem 4.1. (NIRB error estimate for the sensitivities.) Let $A(\mu) = \mu I_d$, with $\mu \in \mathbb{R}_+^+$, and let us consider the problem 3 with its exact solution $u(x, t; \mu)$, and the full discretized solution $u_h^n(x; \mu)$ to the problem 10. Let $\Psi(x, t; \mu)$ and $\Psi_h^n(x; \mu)$ respectively by the corresponding sensitivities, given by (23) and (44). Let $(\zeta_i^h)_{i=1, \dots, N_1}$ be the L^2 -orthonormalized and H^1 -orthogonalized RB generated with the greedy algorithm 1 through the NIRB algorithm 3.1.1. Let us consider the NIRB approximation defined by (95) i.e.

$$\text{for } n = 0, \dots, N_T, \quad \Psi_{Hh}^{N,n}(\mu) := \sum_{i=1}^{N_1} (\widetilde{\Psi}_H^n(\mu), \zeta_i^h) \zeta_i^h,$$

where $\widetilde{\Psi}_H^n(\mu)$ is given by (81). Then, the following estimate holds

$$\forall n = 0, \dots, N_T, \quad \left\| \Psi(t^n)(\mu) - \Psi_{Hh}^{N,n}(\mu) \right\|_{H^1(\Omega)} \leq \varepsilon(N) + C_1(\mu)h + C_2(\mu, N)H^2 + C_3(\mu)\Delta t_F + C_4(\mu, N)\Delta t_G^2, \quad (114)$$

where C_1, C_2, C_3 and C_4 are constants independent of h and H , Δt_F and Δt_G . The term ε depends on the Kolmogorov N -width and measures the error given by (21).

If H is such as $H^2 \sim h$, $\Delta t_G^2 \sim \Delta t_F$, and $C_2(\mu, N)$ and $C_4(\mu, N)$ not too large, it results in an error estimate in $\varepsilon(N) + \mathcal{O}(h + \Delta t_F)$. Theorem 4.1 then states that we recover optimal error estimates in $L^\infty(0, T; H^1(\Omega))$ if $\varepsilon(N)$ is small enough. We now go on with the proof of Theorem 4.1.

Proof. The NIRB approximation at time step $n = 0, \dots, N_T$, for a new parameter $\mu \in \mathcal{G}$ is defined by (95). Thus, the triangle inequality gives

$$\begin{aligned} \left\| \Psi(t^n)(\mu) - \Psi_{Hh}^{N,n}(\mu) \right\|_{H^1(\Omega)} &\leq \left\| \Psi(t^n)(\mu) - \Psi_h^n(\mu) \right\|_{H^1(\Omega)} + \left\| \Psi_h^n(\mu) - \Psi_{hh}^{N,n}(\mu) \right\|_{H^1(\Omega)} + \left\| \Psi_{hh}^{N,n}(\mu) - \Psi_{Hh}^{N,n}(\mu) \right\|_{H^1(\Omega)} \\ &=: T_1 + T_2 + T_3, \end{aligned} \quad (115)$$

where $\Psi_{hh}^{N_1,n}(\mu) = \sum_{i=1}^{N_1} (\Psi_h^n(\mu), \zeta_i^h) \zeta_i^h$.

- The first term T_1 may be estimated using the inequality given by Theorem 2.9, such that

$$\left\| \Psi(t^n)(\mu) - \Psi_h^n(\mu) \right\|_{H^1(\Omega)} \leq C(\mu) (h + \Delta t_F). \quad (116)$$

- We then denote by $\mathcal{S}'_h = \{\Psi_h^n(\mu, t), \mu \in \mathcal{G}, n = 0, \dots, N_T\}$ the set of all the sensitivities. For our model problem, this manifold has a low complexity. It means that for an accuracy $\varepsilon = \varepsilon(N)$ related to the Kolmogorov N -width of the manifold \mathcal{S}'_h , for any $\mu \in \mathcal{G}$, and any $n \in 0, \dots, N_T$, T_2 is bounded by ε which depends on the Kolmogorov N -width.

$$T_2 = \left\| \Psi_h^n(\mu) - \sum_{i=1}^{N_1} (\Psi_h^n(\mu), \zeta_i^h) \zeta_i^h \right\|_{H^1(\Omega)} \leq \varepsilon(N). \quad (117)$$

- Since $(\zeta_i^h)_{i=1, \dots, N_1}$ is a family of L^2 and H^1 orthogonalized RB functions (see [20] for only L^2 orthonormalized RB functions)

$$\left\| \Psi_{hh}^{N,n} - \Psi_{Hh}^{N,n} \right\|_{H^1(\Omega)}^2 = \sum_{i=1}^{N_1} |(\Psi_h^n(\mu) - \widetilde{\Psi}_H^n(\mu), \zeta_i^h)|^2 \left\| \zeta_i^h \right\|_{H^1(\Omega)}^2, \quad (118)$$

where $\widetilde{\Psi}_H^n(\mu)$ is the quadratic interpolation of the coarse snapshots on time t^n , $\forall n = 0, \dots, N_T$, defined by (81). From the RB orthonormalization in L_2 , the equation (106) yields

$$\left\| \zeta_i^h \right\|_{H^1}^2 := \left\| \nabla \zeta_i^h \right\|_{L^2(\Omega)}^2 = \lambda_i \left\| \zeta_i^h \right\|_{L^2(\Omega)}^2 = \lambda_i \leq \max_{i=1, \dots, N} \lambda_i = \lambda_N, \quad (119)$$

such that the equation (118) leads to

$$\left\| \Psi_{hh}^{N,n} - \Psi_{Hh}^{N,n} \right\|_{H^1(\Omega)}^2 \leq C\lambda_N \left\| \Psi_h^n(\mu) - \widetilde{\Psi}_H^n(\mu) \right\|_{L^2(\Omega)}^2. \quad (120)$$

Now by definition of $\widetilde{\Psi}_H^n(\mu)$ and by corollary 2.11 and Theorem 2.8, for $t^n \in I_m$,

$$\left\| \Psi_h^n(\mu) - \widetilde{\Psi}_H^n(\mu) \right\|_{L^2(\Omega)} \leq C(\mu)(H^2 + \Delta t_G^2 + h^2 + \Delta t_F), \quad (121)$$

and we end up for equation (120) with

$$\left\| \Psi_{hh}^{N,n} - \Psi_{Hh}^{N,n} \right\|_{H^1(\Omega)} \leq C(\mu)\sqrt{\lambda_N}(H^2 + \Delta t_G^2 + h^2 + \Delta t_F), \quad (122)$$

where $C(\mu)$ does not depend on N . Combining these estimates (116), (117) and (122) concludes the proof and yields the estimate (114). □

5 Numerical results.

In this section, we have applied the NIRB algorithms on several numerical tests. We have implemented the problem model and the Brusselator system (as our two NIRB applications) using FreeFem++ (version 4.9) [29] to compute the fine and coarse snapshots, and the solutions have been stored in VTK format.

Then we have applied the NIRB algorithms with python (with the library scikit-learn [37] for the GP version), in order to highlight the non-intrusive side of the two-grid method (as in [20]). After saving the NIRB approximations with Paraview module on Python, the errors have been computed with FreeFem++.

5.1 On the heat equation.

In order to validate our numerical results, we have chosen a right-hand side function

$$f(t, \mathbf{x}) = 10[x^2(x-1)^2y^2(y-1)^2 - 2(t+1)((6x^2 - 6x + 1)(y^2(y-1)^2) + (6y^2 - 6y + 1)(x^2(x-1)^2))], \quad (123)$$

such that for $\mu = 1$, we can calculate an analytical solution for u , which is given by

$$u(t, \mathbf{x}; 1) = 10(t+1)x^2(1-x)^2y^2(1-y)^2, \forall t \in [0, 1], \quad (124)$$

where $\mathbf{x} = (x, y) \in [0, 1]^2$. We have solved (3) and (23) on the parameter set $\mathcal{G} = [0.5, 9.5]$. The initial solution $u_0(\mu)$ solves the elliptic equation (with homogeneous Dirichlet boundary conditions)

$$-\mu\Delta u_0 = f_0, \text{ with } f_0(\mathbf{x}) = -20 [(6x^2 - 6x + 1)(y^2(y-1)^2) + (6y^2 - 6y + 1)(x^2(x-1)^2)].$$

We have retrieved several snapshots on $t = [0, 1]$ (note that the coarse time grid must belong to the interval of the fine one), and tried our algorithms on several size of meshes, always with $\Delta t_F \simeq h$ and $\Delta t_G \simeq H$ (both schemes are stables), and such that $h = H^2$.

- Figure 1 illustrates the convergence rates of the FEM and NIRB approximations. We have taken 18 parameters in \mathcal{G} for the RB construction such that $\mu_i = 0.5i$, $i = 1, \dots, 19, i \neq 2$ and a reference solution to problem (44), with $\mu = 1$ and its mesh and time step such that $h_{ref} \simeq \Delta t_{F,ref} = 0.0025$. In Figure 1, we present the H_0^1 relative errors of the FEM solutions on the fine and coarse meshes, and compare them to the ones obtained with the NIRB algorithms (classical NIRB, NIRB with rectification and NIRB with GPR 3.1).
- Then, we have taken 19 parameters in \mathcal{G} for the RB construction such that $\mu_i = 0.5i$, $i = 1, \dots, 19$ and have applied the “leave-one-out” strategy. In order to evaluate the NIRB algorithm with respect to the parameters, table 2 presents the maximum relative H_0^1 -errors between the fine solution $u_h(\mu)$ and the NIRB

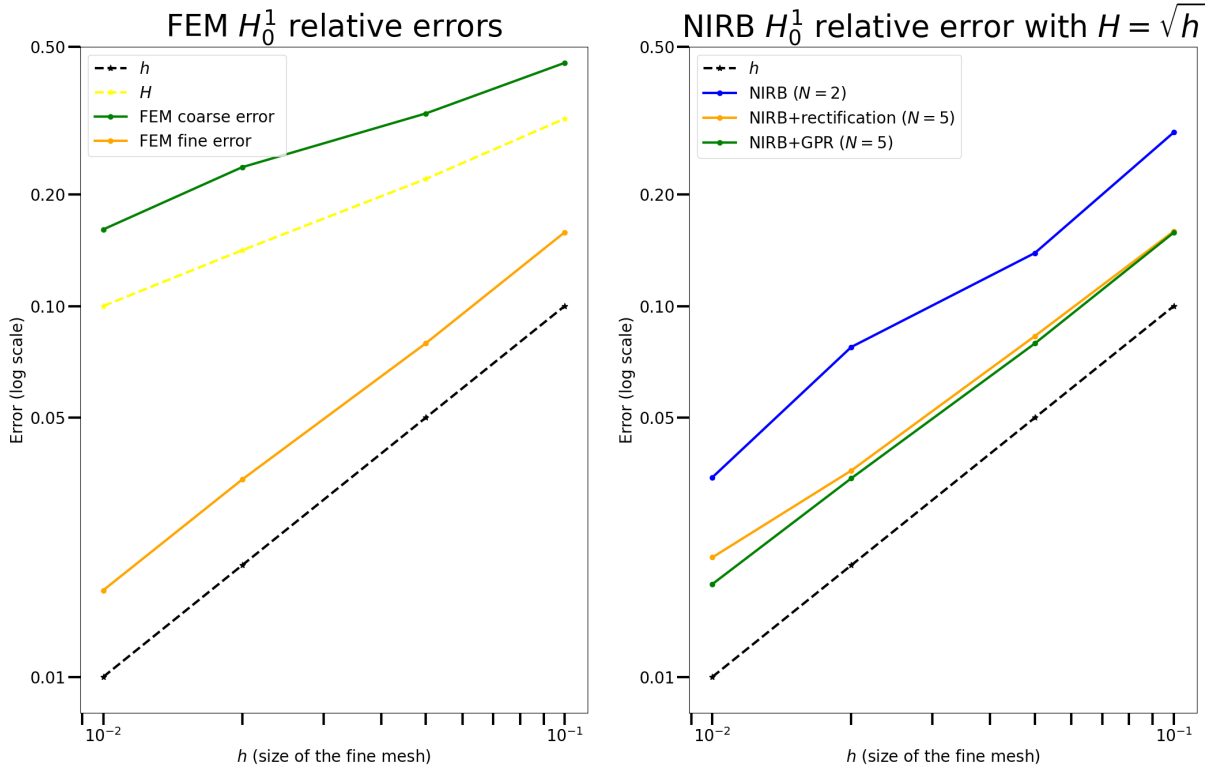


Figure 1: Heat equation: H_0^1 relative FEM errors (left) compared to H_0^1 relative NIRB errors (right) with several $\Delta t_F \simeq h \simeq H^2 \simeq \Delta t_G$ and $\mu = 1$

approximations over the parameters (inside the parameters training set), where $\Psi_{p,h}^{N_p,n}(\mu)$ denotes the true projection on $X_{p,h}^{N_p}$ given by

$$\text{For } n = 0, \dots, N_T, \quad \Psi_{p,h}^{N_p,n}(\mu) := \sum_{i=1}^{N_p} (\Psi_{p,h}^n(\mu), \zeta_{p,i}^h) \zeta_{p,i}^h. \quad (125)$$

In 2, we observe that the error for the worst parameter is divided by 2 in case of the rectified NIRB version (more samples would be necessary to further reduce the error). Moreover, the GP yields very accurate results even in the worst scenario.

Table 1: Maximum H_0^1 error over the parameters (compared to the true projection and to the FEM coarse projection) with $N = 5$ with $h = 0.01 \simeq H^2$

Plain NIRB error	NIRB rectified error	NIRB GP error	$\max_{\mu \in \mathcal{G}_{train}} \frac{\ \Psi_{p,h}(\mu) - \Psi_{p,h}^{N_p}(\mu)\ _{l^\infty(0,\dots,N_T;H_0^1(\Omega))}}{\ \Psi_{p,h}(\mu)\ _{l^\infty(0,\dots,N_T;H_0^1(\Omega))}}$	$\max_{\mu \in \mathcal{G}_{train}} \frac{\ \Psi_{p,h}(\mu) - \Psi_{p,H}(\mu)\ _{l^\infty(0,\dots,N_T;H_0^1(\Omega))}}{\ \Psi_{p,h}(\mu)\ _{l^\infty(0,\dots,N_T;H_0^1(\Omega))}}$
1.3×10^{-1}	8.8×10^{-2}	6.6×10^{-4}	5.7×10^{-6}	1.9×10^{-1}

5.2 On the Brusselator system.

The Brusselator problem [42] involves chemical reactions. It is a more complex test from a simulation point of view than the heat equation due to a nonlinearity. The chemical concentrations u_1 and u_2 are controlled by parameters $\mu = (a, b, \alpha)$ throughout the reaction process, making it an interesting application of a NIRB method in the context of sensitivity analysis.

Let us consider as the spatial domain $\Omega = [0, 1]^2$. The nonlinear system of this two-dimensional reaction-diffusion problem with $\mathbf{u} = (u_1, u_2)$ writes:

$$\begin{cases} \partial_t u_1 = F_1(\mathbf{u}) := a + u_1^2 u_2 - (b+1)u_1 + \alpha \Delta u_1, & \text{in } \Omega \times]0, T] \\ \partial_t u_2 = F_2(\mathbf{u}) := b u_1 - u_1^2 u_2 + \alpha \Delta u_2, & \text{in } \Omega \times]0, T], \\ u_1(\mathbf{x}, 0) = u^0(\mathbf{x}) = 2 + 0.25y, & \text{in } \Omega \\ u_2(\mathbf{x}, 0) = v_0(\mathbf{x}) = 1 + 0.8x, & \text{in } \Omega, \\ \partial_n u_1 = 0, & \partial\Omega, \\ \partial_n u_2 = 0, & \partial\Omega. \end{cases}$$

Our parameter, denoted $\mu = (a, b, \alpha)$, belongs to $[2, 4] \times [1, 4] \times [0.001, 0.05]$. We have taken an ending time $T = 4$. These parameters are standard. We note that for $b \leq 1 + a^2$ the solutions are stable, and for α small enough they converge to $(u_l, v_l) = (a, \frac{b}{a})$.

We use an Euler implicit scheme for fine solutions and fine sensitivities with the Newton algorithm to deal with nonlinearity and Crank-Nicolson scheme for the coarse mesh.

Thus we have taken $a = 2, 2.5, 4$, $b = 1, 3, 4$ and $\alpha = 0.001, 0.01, 0.05$, and have tested our NIRB algorithms on the new parameter $(a, b, \alpha) = (3, 2, 0.008)$ with $h = 0.02 = \Delta t_F \simeq H^2 = \Delta t_G^2$ ($H = 0.14$).

- We plot the three coarse FEM sensitivity $L^\infty(\Omega)$ relative errors with respect to time in Figure 2, and compare them to the ones obtain with the rectification post-treatment and with the new GP algorithm with $N = 20$. We remark that we gain a factor of 10 with the GP process regression compared to the FEM coarse error for the parameters a and b in average, and for the rectified version a factor of 50. The results on the diffusion coefficient α are less accurate for both methods. It comes from the fact that the diffusion sensitivity is harder to capture for these parameter values as we remark in Figure 3 with the $L^\infty(\Omega)$ error obtained from the true projection defined by (125), which is of same order as the coarse FEM error given in Figure 2.
- Then, we have tested the NIRB algorithm with the adjoint formulation 3.2 where we have used as the objective function $\mathcal{F}(\mu) = \frac{1}{2} \sum_{n=0}^{N_T} \|\mathbf{u}_h^n(\mu) - \bar{\mathbf{u}}^n\|_{L^2(\Omega)}^2$ as in (82) (or (83) in its continuous version). We have

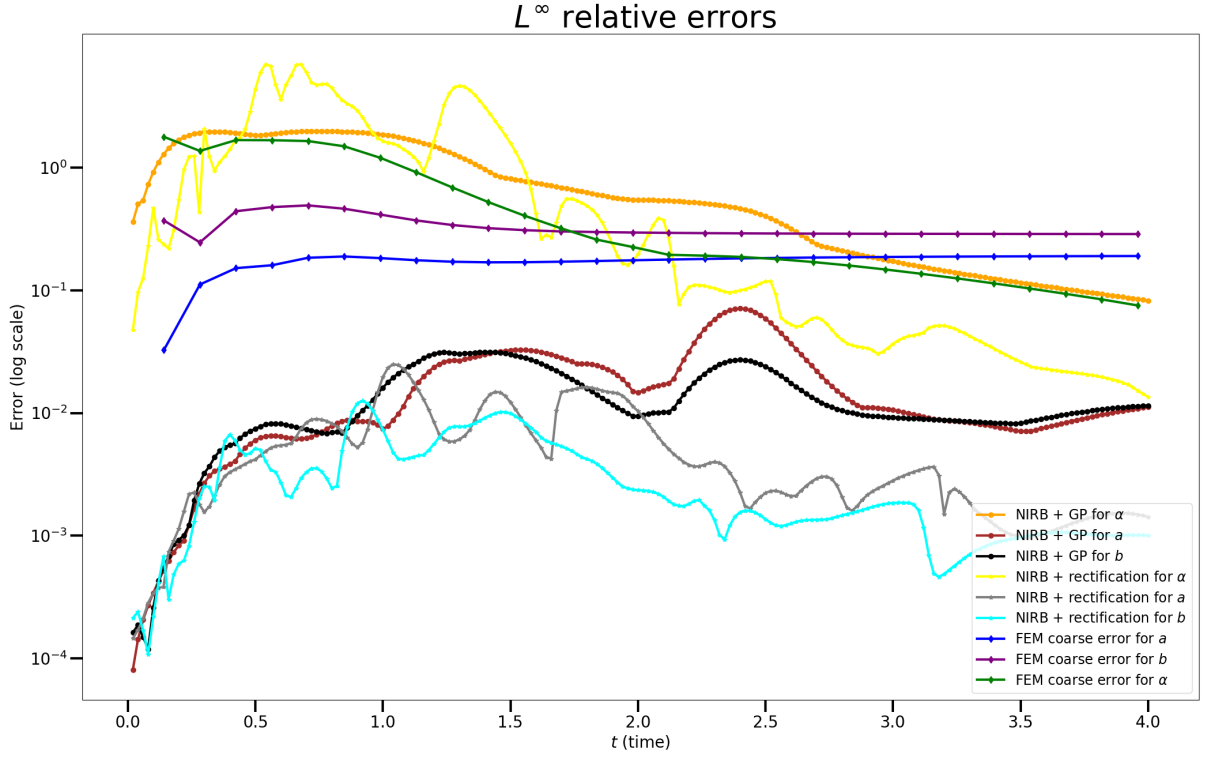


Figure 2: Sensitivities $L^\infty(\Omega)$ relative errors with respect to time $t = [0, 4]$, with a new parameter $(a, b, \alpha) = (3, 2, 0.008)$, in $\Omega = [0, 1]^2$ (NIRB GP version / NIRB rectified version compared to fine sensitivities)

added noise for the measures $\bar{\mathbf{u}}^n$. We display in Table 2 the values of $\frac{\partial \mathcal{F}}{\partial a}(\mu)$ with the fine sensitivities (respectively with b and α) and compare them with the NIRB ones given by (113). Now, the Lagrangian for the Brusselator system with $\chi = (\chi_1, \chi_2)$ as our lagrangian multiplier takes the form:

$$\mathcal{L}(\mathbf{u}, \chi; \mu) = \mathcal{F}(\mu) + \int_0^T (\chi_1, F_1(\mathbf{u}) - u_{1t}) + (\chi_2, F_2(\mathbf{u}) - u_{2t}) \, ds. \quad (126)$$

Following the same steps as for the heat equation in A, we obtain the following associated adjoint system (in its continuous version)

$$\left\{ \begin{array}{l} \chi_{1t} = -\frac{\partial \text{err}}{\partial u_1} - 2u_1 u_2 \chi_1 + (b+1)\chi_1 - \alpha \Delta \chi_1 - b\chi_2 + 2u_1 u_2 \chi_2, \text{ in } \Omega \times [0, T[, \\ \chi_{2t} = -\frac{\partial \text{err}}{\partial u_2} - \chi_1 u_1^2 + \chi_2 u_1^2 - \alpha \Delta \chi_2, \text{ in } \Omega \times [0, T[, \\ \chi_1(\cdot, T) = 0, \text{ in } \Omega, \\ \chi_2(\cdot, T) = 0, \text{ in } \Omega, \\ \partial_n \chi_1(\cdot, t) = 0, \text{ on } \partial\Omega \times [0, T[, \\ \partial_n \chi_2(\cdot, t) = 0, \text{ on } \partial\Omega \times [0, T[. \end{array} \right. \quad (127)$$

5.2.1 Time execution (min,sec)

Finally, the computational costs are well saved during the online part of these NIRB algorithms as it is highlighted with this example ($h = 0.02$ and $H = 0.14$). We present the FEM for one instance of parameter in tables 3 and the NIRB runtimes with the adjoint rectified version 4 and the GP NIRB approach 5.

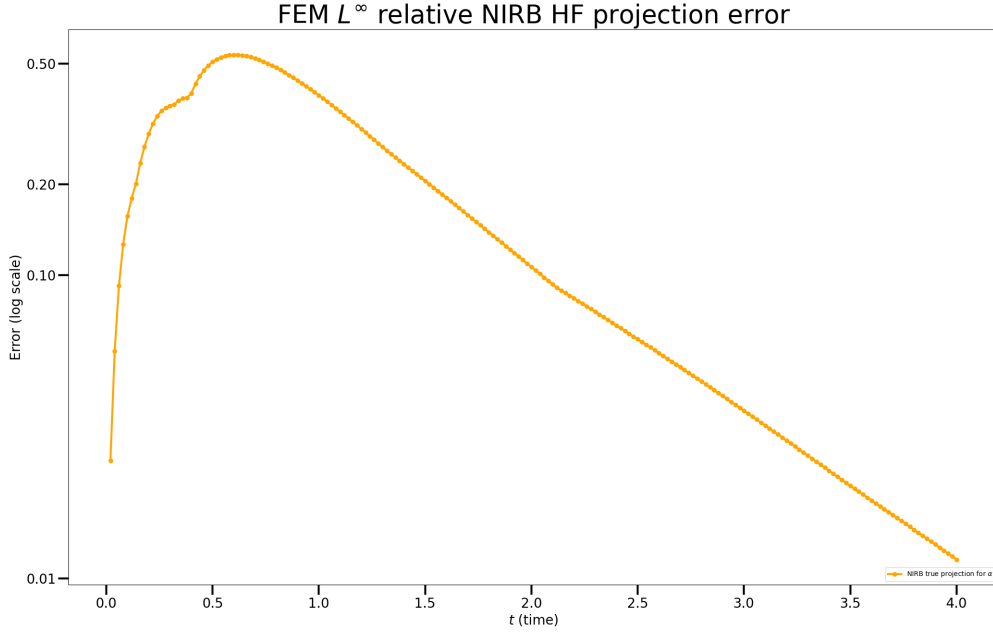


Figure 3: Sensitivities $L^\infty(\Omega)$ relative errors with respect to time $t = [0, 4]$, with a new parameter $(a, b, \alpha) = (3, 2, 0.008)$, in $\Omega = [0, 1]^2$: diffusion sensitivity (parameter α) NIRB HF projection

Table 2: Objective sensitivity values with $N = 5$ with $h = 0.02 \simeq H^2$

Parameter	High-Fidelity values	rectified NIRB adjoint version
a	-2.74×10^{-6}	4.97×10^{-3}
b	1.17×10^{-5}	1.66×10^{-2}
α	-6.73×10^{-4}	-3.54×10^{-2}

Table 3: FEM runtimes (min:sec)

FEM high fidelity solver	FEM coarse solution
01:20	00:02

Table 4: NIRB rectified runtimes ($N = 30$, min:sec)

NIRB Offline	rectified NIRB online
58:00	04:00

Table 5: NIRB GP runtimes ($N = 30$, h:min:sec)

NIRB Offline	GP NIRB online
1:02:00	00:04:00

A Derivation of the adjoint for the heat equation.

In this appendix, we recall the main steps to derive the adjoint of our model problem, in order to compute $(\frac{\partial \mathcal{F}}{\partial \mu_k})_{k=1,\dots,P}$. For a more general problem, we refer to [50] in case of FEM.

- We consider the Lagrangian formulation (84), denoted by \mathcal{L} .
- Differentiating \mathcal{L} with respect to the parameter μ_p , for $p = 1, \dots, P$, we obtain

$$\frac{d\mathcal{L}}{d\mu_p}(u, \chi, \zeta; \mu) = \int_0^T \left[\int_{\Omega} \frac{derr}{d\mu_p}(\mu) dx + \left(\chi, \frac{d[\nabla \cdot (A(\mu)\nabla u) + f - u_t]}{d\mu_p} \right) \right] ds. \quad (128)$$

In our setting, the objective does not depend directly on the parameter μ_p . The time and the parameter derivatives can commute $(\frac{d}{dt}(\frac{du}{d\mu_p}) = \frac{d}{d\mu_p}(\frac{du}{dt}))$, and since f is independent of μ , the term linked to f vanishes. Therefore, using the chain rule, it may be rewritten

$$\frac{d\mathcal{L}}{d\mu_p}(u, \chi, \zeta; \mu) = \int_0^T \left[\left(\frac{\partial err}{\partial u}, \Psi_p \right) + \left(\chi, \nabla \cdot \left(\frac{\partial A}{\partial \mu_p}(\mu) \nabla u \right) \right) + \left(\chi, \frac{\partial[\nabla \cdot (A(\mu)\nabla u)]}{\partial u} \Psi_p \right) - \underbrace{\left(\chi, \Psi_{p,t} \right)}_{T_{IBP}} \right] ds, \quad (129)$$

where

$$\Psi_p(t, \mathbf{x}; \mu) := \frac{\partial u}{\partial \mu_p}(t, \mathbf{x}; \mu).$$

As we saw before, a classical forward sensitivity computation would require $P + 1$ systems of PDEs to solve. Here, we want to avoid calculating the sensitivities of the state variables. To do so, the strategy of the adjoint method is to factorize all the terms depending on Ψ_p , and to impose them to vanish by adequately choosing χ (which is arbitrary). By IBP on T_{IBP} ,

$$\int_0^T \int_{\Omega} \chi \cdot \Psi_{p,t} dx ds = \int_{\Omega} [\chi(T) \cdot \Psi_p(T) - \chi(0) \cdot \Psi_p(0)] dx - \int_0^T \int_{\Omega} \chi_t \cdot \Psi_p dx ds,$$

and choosing $\chi(T) = 0$, it yields

$$\frac{d\mathcal{L}}{d\mu_p}(u, \chi, \zeta; \mu) = \int_0^T \left[\left(\frac{\partial err}{\partial u}, \Psi_p \right) + \left(\chi, \nabla \cdot \left(\frac{\partial A}{\partial \mu_p}(\mu) \nabla u \right) \right) + \left(\chi, \frac{\partial[\nabla \cdot (A(\mu)\nabla u)]}{\partial u} \Psi_p \right) + \left(\chi_t, \Psi_p \right) \right] ds + \chi(0) \cdot \Psi_p(0).$$

Thus, we want the following term to vanish

$$\int_0^T \int_{\Omega} \left[\frac{\partial err}{\partial u} \cdot \Psi_p + \underbrace{\chi \frac{\partial[\nabla \cdot (A(\mu)\nabla u)]}{\partial u} \cdot \Psi_p}_{T_{GF}} + \chi_t \cdot \Psi_p \right] dx ds. \quad (130)$$

Now, applying Green's formula twice, we have

$$\begin{aligned} \int_0^T \int_{\Omega} T_{GF} dx ds &= \int_0^T \int_{\Omega} \chi \nabla \cdot (A(\mu) \nabla \Psi_p) dx ds = \int_0^T \left[- \int_{\Omega} A(\mu) \nabla \chi \cdot \nabla \Psi_p dx + \int_{\partial\Omega} A(\mu) \chi \cdot \nabla_n \Psi_p d\sigma \right] ds, \\ &= \int_0^T \left[\int_{\Omega} \nabla \cdot (A(\mu) \nabla \chi) \cdot \Psi_p dx - \int_{\partial\Omega} A(\mu) \nabla_n \chi \cdot \Psi_p d\sigma + \int_{\partial\Omega} A(\mu) \chi \cdot \nabla_n \Psi_p d\sigma \right] ds, \end{aligned}$$

with $\nabla_n(\cdot)$ the normal derivative. Therefore, from the initial boundary conditions, since $\forall t \geq 0, \forall \mu \in \mathcal{G}$, $u(t) = 0$ on $\partial\Omega$, we also have $\Psi_p(t) = 0$ on $\partial\Omega$ and by imposing $\chi = 0$ on $\partial\Omega$, (130) becomes

$$\int_0^T \int_{\Omega} \left[\left(\frac{\partial err}{\partial u} + \nabla \cdot (A(\mu) \nabla \chi) + \chi_t \right) \cdot \Psi_p \right] dx ds = 0,$$

and this equation leads us to the following adjoint state problem

$$\left\{ \begin{array}{l} \text{Find } \chi \in V \text{ such that} \\ \chi_t = -\frac{\partial err}{\partial u} - \nabla \cdot (A(\mu) \nabla \chi), \text{ in } \Omega \times [0, T[, \\ \chi(\mathbf{x}, T) = 0, \text{ in } \Omega, \\ \chi(\mathbf{x}, t) = 0, \text{ on } \partial\Omega \times [0, T[. \end{array} \right. \quad (131)$$

Acknowledgment

This work is supported by the SPP2311 program. We would like to give special thanks to Ole Burghardt for his precious help on Automatic Differentiation.

References

- [1] E. Bader, M. Kärcer, M. A. Grepl, and K. Veroy. Certified reduced basis methods for parametrized distributed elliptic optimal control problems with control constraints. *SIAM Journal on Scientific Computing*, 38(6):A3921–A3946, 2016.
- [2] M. Barrault, C. Nguyen, A. Patera, and Y. Maday. An ‘empirical interpolation’ method: application to efficient reduced-basis discretization of partial differential equations. *Comptes rendus de l’Académie des sciences. Série I, Mathématique*, 339-9:667–672, 2004.
- [3] P. Binev, A. Cohen, W. Dahmen, R. DeVore, G. Petrova, and P. Wojtaszczyk. Convergence rates for greedy algorithms in reduced basis methods. *SIAM journal on mathematical analysis*, 43(3):1457–1472, 2011.
- [4] E. Borgonovo and E. Plischke. Sensitivity analysis: a review of recent advances. *European Journal of Operational Research*, 248(3):869–887, 2016.
- [5] S. Brenner and R. Scott. *The mathematical theory of finite element methods*, volume 15. Springer Science & Business Media, 2007.
- [6] F. Casenave, A. Ern, and T. Lelièvre. A nonintrusive reduced basis method applied to aeroacoustic simulations. *Advances in Computational Mathematics*, 41(5):961–986, Jun 2014.
- [7] R. Chakir and Y. Maday. A two-grid finite-element/reduced basis scheme for the approximation of the solution of parametric dependent p.d.e. In *9e Colloque national en calcul des structures*, 2009.
- [8] R. Chakir, B. Streichenberger, and P. Chatellier. A non-intrusive reduced basis method for urban flows simulation. *14th WCCM-ECCOMAS Congress 2020*, 2020.
- [9] P. Chen, A. Quarteroni, and G. Rozza. Reduced basis methods for uncertainty quantification. *SIAM/ASA Journal on Uncertainty Quantification*, 5(1):813–869, 2017.
- [10] A. Cohen, M. Dolbeault, O. Mula, and A. Somacal. Nonlinear approximation spaces for inverse problems. *arXiv preprint arXiv:2209.09314*, 2022.
- [11] L. Dede. Reduced basis method and a posteriori error estimation for parametrized linear-quadratic optimal control problems. *SIAM Journal on Scientific Computing*, 32(2):997–1019, 2010.
- [12] L. Dedè. Reduced basis method and error estimation for parametrized optimal control problems with control constraints. *Journal of Scientific Computing*, 50(2):287–305, 2012.
- [13] Z. Ding, J. Shi, Q. Gao, Q. Huang, and W-H. Liao. Design sensitivity analysis for transient responses of viscoelastically damped systems using model order reduction techniques. *Structural and Multidisciplinary Optimization*, 64(3):1501–1526, 2021.
- [14] David Duvenaud. *Automatic model construction with Gaussian processes*. PhD thesis, University of Cambridge, 2014.
- [15] L. C. Evans. *Partial differential equations*. American Mathematical Society, Providence, R.I., 2010.
- [16] R. Geelen, S. Wright, and K. Willcox. Operator inference for non-intrusive model reduction with nonlinear manifolds. *arXiv preprint arXiv:2205.02304*, 2022.
- [17] D. Givoli. A tutorial on the adjoint method for inverse problems. *Computer Methods in Applied Mechanics and Engineering*, 380:113810, 2021.
- [18] E. Grosjean and Y. Maday. Error estimate of the non-intrusive reduced basis method with finite volume schemes. *ESAIM: M2AN*, 55(5):1941–1961, 2021.

- [19] E. Grosjean and Y. Maday. A doubly reduced approximation for the solution to pde's based on a domain truncation and a reduced basis method: Application to navier-stokes equations. *preprint hal-03588508*, 2022.
- [20] E. Grosjean and Y. Maday. Error estimate of the non-intrusive reduced basis (nirb) two-grid method with parabolic equations. *arXiv preprint arXiv:2211.08897*, 2022.
- [21] Mengwu Guo and Jan S. Hesthaven. Reduced order modeling for nonlinear structural analysis using gaussian process regression. *Computer Methods in Applied Mechanics and Engineering*, 341:807–826, 2018.
- [22] Mengwu Guo and Jan S Hesthaven. Data-driven reduced order modeling for time-dependent problems. *Computer methods in applied mechanics and engineering*, 345:75–99, 2019.
- [23] B. Haasdonk. Convergence rates of the pod–greedy method. *ESAIM: Mathematical modelling and numerical Analysis*, 47(3):859–873, 2013.
- [24] B. Haasdonk and M. Ohlberger. Reduced basis method for finite volume approximations of parametrized linear evolution equations. *ESAIM: Mathematical Modelling and Numerical Analysis-Modélisation Mathématique et Analyse Numérique*, 42(2):277–302, 2008.
- [25] J. K. Hammond, R. Chakir, F. Bourquin, and Y. Maday. Pbdw: A non-intrusive reduced basis data assimilation method and its application to an urban dispersion modeling framework. *Applied Mathematical Modelling*, 76:1–25, 2019.
- [26] A. Hay, I. Akhtar, and J. T Borggaard. On the use of sensitivity analysis in model reduction to predict flows for varying inflow conditions. *International Journal for Numerical Methods in Fluids*, 68(1):122–134, 2012.
- [27] A. Hay, J. Borggaard, I. Akhtar, and D. Pelletier. Reduced-order models for parameter dependent geometries based on shape sensitivity analysis. *Journal of computational Physics*, 229(4):1327–1352, 2010.
- [28] A. Hay, J. T. Borggaard, and D. Pelletier. Local improvements to reduced-order models using sensitivity analysis of the proper orthogonal decomposition. *Journal of Fluid Mechanics*, 629:41–72, 2009.
- [29] F. Hecht. New development in freefem++. *Journal of numerical mathematics*, 20(3-4):251–266, 2012.
- [30] K Ito and S. S Ravindran. A reduced basis method for control problems governed by pdes. In *Control and estimation of distributed parameter systems*, pages 153–168. Springer, 1998.
- [31] A. Janon, Ma. Nodet, and C. Prieur. Goal-oriented error estimation for the reduced basis method, with application to sensitivity analysis. *Journal of Scientific Computing*, 68(1):21–41, 2016.
- [32] M. Kärcher, Z. Tokoutsis, M. A Grepl, and K. Veroy. Certified reduced basis methods for parametrized elliptic optimal control problems with distributed controls. *Journal of Scientific Computing*, 75(1):276–307, 2018.
- [33] U. Kirsch. Reduced basis approximations of structural displacements for optimal design. *AIAA journal*, 29(10):1751–1758, 1991.
- [34] U. Kirsch. Efficient sensitivity analysis for structural optimization. *Computer Methods in Applied Mechanics and Engineering*, 117(1):143–156, 1994.
- [35] D J. Knezevic and A T. Patera. A certified reduced basis method for the fokker–planck equation of dilute polymeric fluids: Fene dumbbells in extensional flow. *SIAM Journal on Scientific Computing*, 32(2):793–817, 2010.
- [36] A. Kolmogoroff. Über die beste annäherung von funktionen einer gegebenen funktionenklasse. *Annals of Mathematics*, pages 107–110, 1936.
- [37] Oliver Kramer. Scikit-learn. In *Machine learning for evolution strategies*, pages 45–53. Springer, 2016.
- [38] D. Kumar, M. Raisee, and C. Lacor. An efficient non-intrusive reduced basis model for high dimensional stochastic problems in cfd. *Computers & Fluids*, 138:67–82, 2016.
- [39] J-L Lions and E Magenes. *Problèmes aux limites non homogènes. II*, volume 11. Annales de l’institut Fourier, 1961.

- [40] Y. Maday. Reduced basis method for the rapid and reliable solution of partial differential equations. *International Congress of Mathematicians Madrid 2006 Volume III. Invited Lectures*, pages 1255–1270, 2006.
- [41] Y. Maday, T Anthony, J. D Penn, and M. Yano. Pbdw state estimation: Noisy observations; configuration-adaptive background spaces; physical interpretations. *ESAIM: Proceedings and Surveys*, 50:144–168, 2015.
- [42] R.C. Mittal and R. Jiware. Numerical solution of two-dimensional reaction–diffusion brusselator system. *Applied Mathematics and Computation*, 217(12):5404–5415, 2011.
- [43] F. Negri, G. Rozza, A. Manzoni, and A. Quarteroni. Reduced basis method for parametrized elliptic optimal control problems. *SIAM Journal on Scientific Computing*, 35(5):A2316–A2340, 2013.
- [44] Ngoc Cuong Nguyen and Jaime Peraire. Gaussian functional regression for output prediction: Model assimilation and experimental design. *Journal of Computational Physics*, 309:52–68, 2016.
- [45] AK Noor, JA Tanner, and JM Peters. Reduced basis technique for evaluating sensitivity derivatives of the nonlinear response of the space shuttle orbiter nose-gear tire. *Tire Science and Technology*, 21(4):232–259, 1993.
- [46] J. S Peterson. The reduced basis method for incompressible viscous flow calculations. *SIAM Journal on Scientific and Statistical Computing*, 10(4):777–786, 1989.
- [47] A. Quarteroni, G. Rozza, and A. Quaini. Reduced basis methods for optimal control of advection-diffusion problems. Technical report, RAS and University of Houston, 2007.
- [48] S. S Ravindran. A reduced-order approach for optimal control of fluids using proper orthogonal decomposition. *International journal for numerical methods in fluids*, 34(5):425–448, 2000.
- [49] B. Streichenberger. *Approches multi-fidélités pour la simulation rapide d’écoulements d’air en milieu urbain*. PhD thesis, 2021. Thèse de doctorat, Université Gustave Eiffel.
- [50] JF Sykes and JL Wilson. Adjoint sensitivity theory for the finite element method. In *Finite Elements in Water Resources*, pages 3–12. Springer, 1984.
- [51] V. Thomée. *Galerkin finite element methods for parabolic problems*, volume 25. Springer Science & Business Media, 2007.
- [52] T. Tonn, K. Urban, and S. Volkwein. Comparison of the reduced-basis and pod a posteriori error estimators for an elliptic linear-quadratic optimal control problem. *Mathematical and Computer Modelling of Dynamical Systems*, 17(4):355–369, 2011.
- [53] B. C Watson and A. K Noor. Sensitivity analysis for large-deflection and postbuckling responses on distributed-memory computers. *Computer methods in applied mechanics and engineering*, 129(4):393–409, 1996.
- [54] Barbara Wirthl, Sebastian Brandstaeter, Jonas Nitzler, Bernhard A Schrefler, and Wolfgang A Wall. Global sensitivity analysis based on gaussian-process metamodeling for complex biomechanical problems. *arXiv preprint arXiv:2202.01503*, 2022.